antioxidants

MDPI

Article

Dose–Time Effects of Dietary Nano-Selenium on Growth, Antioxidant Capacity, and Selenoprotein Expression in Juvenile Large-Scale Loach (*Paramisgurnus dabryanus*)

Zhihui Huang [1], Benhe Ma [2], Xin'an Wang [1], Ruiyu Deng [1], Qi Liu [1], Guohong Yu [2], Guohua Ke [3], Haihua Wang [2,*] and Aijun Ma [1,*]

[1] State Key Laboratory of Mariculture Biobreeding and Sustainable Goods, China-ASEAN Belt and Road Joint Laboratory on Mariculture Technology (Qingdao), Yellow Sea Fisheries Research Institute, Chinese Academy of Fishery Sciences, Qingdao 266071, China; huangzh@ysfri.ac.cn (Z.H.)
[2] Jiangxi Fisheries Research Institute, Nanchang 330039, China; mabenhe@126.com (B.M.)
[3] Jiujiang Xingxiang Aquatic Breeding Co., Ltd., Jiujiang 332200, China
* Correspondence: jxswhh@163.com (H.W.); maaj@ysfri.ac.cn (A.M.); Tel.: +86-0791-88101682 (H.W.); +86-0532-85835103 (A.M.)

Abstract

Selenium (Se) is an essential trace element for aquatic animals, but its narrow margin between nutritional requirement and toxicity necessitates precise supplementation strategies. Nano-selenium (Nano-Se) has emerged as a promising alternative, yet its dose- and time-dependent effects on the *Paramisgurnus dabryanus* remain poorly understood. This study employed a central composite design (CCD) within response-surface methodology (RSM) to systematically investigate the interactive effects of dietary Nano-Se concentration (0–4 mg Se/kg diet) and feeding duration (20–60 days) on growth performance, and further evaluated hepatic antioxidant parameters as well as expression profiles of 12 selenoprotein- and glutathione-metabolism-related genes. The RSM models for weight-gain rate (WGR) and specific growth rate (SGR) were highly significant (R^2_Adj = 0.972 and 0.855, respectively; $p < 0.001$), revealing that the two factors act independently (TS term not significant, $p > 0.05$). Optimal growth was achieved at 1.0 mg/kg Nano-Se, with feeding duration showing a continuous positive effect on WGR (maximum at 60 d) but a plateau effect on SGR after 30 days. The medium dose (1.0 mg/kg) maintained stable antioxidant capacity and induced the strongest gene–enzyme coupling at 40 days (e.g., selenoprotein O1 (selenoo1) vs. SOD: $\varrho = 0.90$, $p < 0.001$). The low dose (0.5 mg/kg) suppressed SOD and GSH-Px activities, whereas the high dose (3.0 mg/kg) disrupted positive coupling and caused an "uncoupling" phenomenon with up-regulation of antioxidant enzymes but down-regulation of transaminases. Twelve functional genes were clustered into three response modules: selenoprotein synthesis (Cluster I, including glutathione peroxidase 1 (gpx1) and tRNA-selenocysteine-1-associated protein (trnau1ap)), GSH-dependent secondary defense (Cluster II), and GSH regeneration/metabolism (Cluster III). Notably, gpx1 and other antioxidant-defense genes were prioritized under adequate Se supply, whereas trnau1ap (SECp43), a potential master switch for selenoprotein translation, was globally down-regulated under long-term high-Se exposure. In conclusion, the optimal Nano-Se supplementation for juvenile *P. dabryanus* is 1.0 mg/kg for 40 days, providing a theoretical basis for precision selenium nutrition in farmed fish.

Academic Editor: Evangelos Zoidis

Received: 13 September 2026
Revised: 16 October 2026
Accepted: 22 October 2026
Published: 27 October 2026

Copyright: © 2026 by the author. Licensee MDPI, Basel, Switzerland. This article is an open access article distributed under the terms and conditions of the Creative Commons Attribution (CC BY) license.

Keywords: nano-selenium; *Paramisgurnus dabryanus*; growth performance; antioxidant capacity; selenoprotein

1. Introduction

Selenium (Se) is an indispensable micronutrient for aquatic animals, playing vital roles in maintaining health, regulating the antioxidant defense system, and promoting growth performance [1,2]. Selenoproteins, particularly glutathione peroxidases (GPx) and thioredoxin reductases, constitute the molecular foundation of Se's biological functions, as they participate directly in scavenging reactive oxygen species and maintaining cellular-redox homeostasis. Dietary Se deficiency has been shown to impair antioxidant capacity and compromise immune function across multiple aquaculture species [3]. Conversely, excessive Se intake can induce oxidative stress and exert toxic effects, reflecting a narrow margin between nutritional requirement and toxicity [2]. The U-shaped dose-response relationship of Se necessitates precise supplementation strategies tailored to specific species and rearing conditions [4].

Traditional inorganic Se sources, such as sodium selenite, exhibit relatively low bioavailability and carry a high risk of toxicity when supplemented at elevated levels [5,6]. Organic Se sources, such as selenomethionine (SeMet) and selenized yeast (Se-yeast), also have adequate bioavailability in fish, with Se-yeast typically containing selenocysteine and/or methylselenocysteine as the major Se species [7,8]. However, their production costs and variable Se content limit their application. Nano-selenium (Nano-Se), defined as elemental selenium nanoparticles (SeNPs), offers a high surface-area-to-volume ratio, enhanced bioavailability, and improved safety profile, making it a promising alternative for precise Se supplementation in aquafeeds [2,9]. Nano-Se supplementation has been consistently shown to promote growth performance, up-regulate the expression of genes encoding antioxidant enzymes and immune-related factors, and enhance disease resistance in various fish species [1,10]. In particular, biosynthesized Nano-Se can optimize gut-microbial composition, activate antioxidant enzyme systems, and modulate immune-related gene expression, thereby significantly improving the health status of aquatic animals [3,9]. Collectively, these findings underscore the potential of Nano-Se as an efficient and safe functional additive in aquaculture nutrition. Nevertheless, the metabolic responses to Nano-Se vary markedly among different aquaculture species, and the optimal dietary dosage as well as the underlying mechanisms remain to be systematically clarified [4].

The large-scale loach (*Paramisgurnus dabryanus*), belonging to the family Cobitidae and subfamily Cobitinae, is a benthic fish characterized by high protein and low lipid content [11]. As an indigenous and economically important freshwater fish in China, it is valued for its tender meat, rich nutrition, strong environmental adaptability, and increasingly mature farming technologies, making it a leading species in the aquaculture industry [12]. With the intensification of culture practices, how to enhance disease resistance, improve flesh quality, and achieve healthy aquaculture through nutritional regulation has become a pressing issue. As a key functional trace element, Se is gaining importance in the health management of *P. dabryanus* [1,2].

Recent studies have made progress in understanding Se nutrition in fish, but most have focused on phenotypic parameters such as growth and antioxidant status [5,7]. However, several key questions remain unanswered: (1) The biological effects of Nano-Se are not only dose-dependent but also time-dependent; however, conventional single-factor experiments fail to reveal the interactive effects between dietary Se concentration and feeding duration. (2) The molecular mechanisms by which Nano-Se regulates the transcriptional expression of Se-metabolism-related genes remain insufficiently explored.

https://doi.org/10.3390/antiox15111392

Previous molecular studies have shown that Nano-Se supplementation can up-regulate GPx1a expression in rainbow trout [13], improve liver health in grass carp [14], and that high Se levels can down-regulate trnau1ap and related selenoprotein genes in yellow catfish [15]. Nevertheless, these studies were mostly limited to single doses or time points, and the dynamic expression patterns of Se-metabolism-related genes under different dose–time combinations remain unknown. (3) The Nano-Se nutritional requirements and molecular response mechanisms of *P. dabryanus*, an economically important freshwater fish in China, have not been reported.

To address these gaps, the present study employed response-surface methodology (RSM) with a central-composite design (CCD) to systematically investigate the interactive effects of dietary Nano-Se level and feeding time on growth performance (weight-gain rate, WGR; specific growth rate, SGR) of *P. dabryanus*. Furthermore, we examined the dynamic changes in hepatic antioxidant parameters (total antioxidant capacity T-AOC, superoxide dismutase SOD, glutathione peroxidase GSH-Px, aspartate aminotransferase AST, alanine aminotransferase ALT, lactate dehydrogenase LDH) and the expression profiles of key genes involved in selenoprotein synthesis and glutathione metabolism. The present study contributes to the field in three main ways: (1) it systematically evaluates the dose–time interactive effects of Nano-Se in *P. dabryanus*; (2) it applies RSM/CCD to optimize Nano-Se supplementation in this species, thereby extending this approach to a new aquaculture species; and (3) it systematically analyzes the expression of 12 selenoprotein- and glutathione metabolism-related genes, revealing a potential "priority hierarchy" in selenoprotein translation. Collectively, these analyses are expected to elucidate the dose- and time-dependent regulatory patterns of Nano-Se at both the phenotypic and molecular levels, providing a theoretical basis and molecular insights for precise selenium nutrition strategies in farmed fish. An overview of the experimental design is shown in Figure 1.

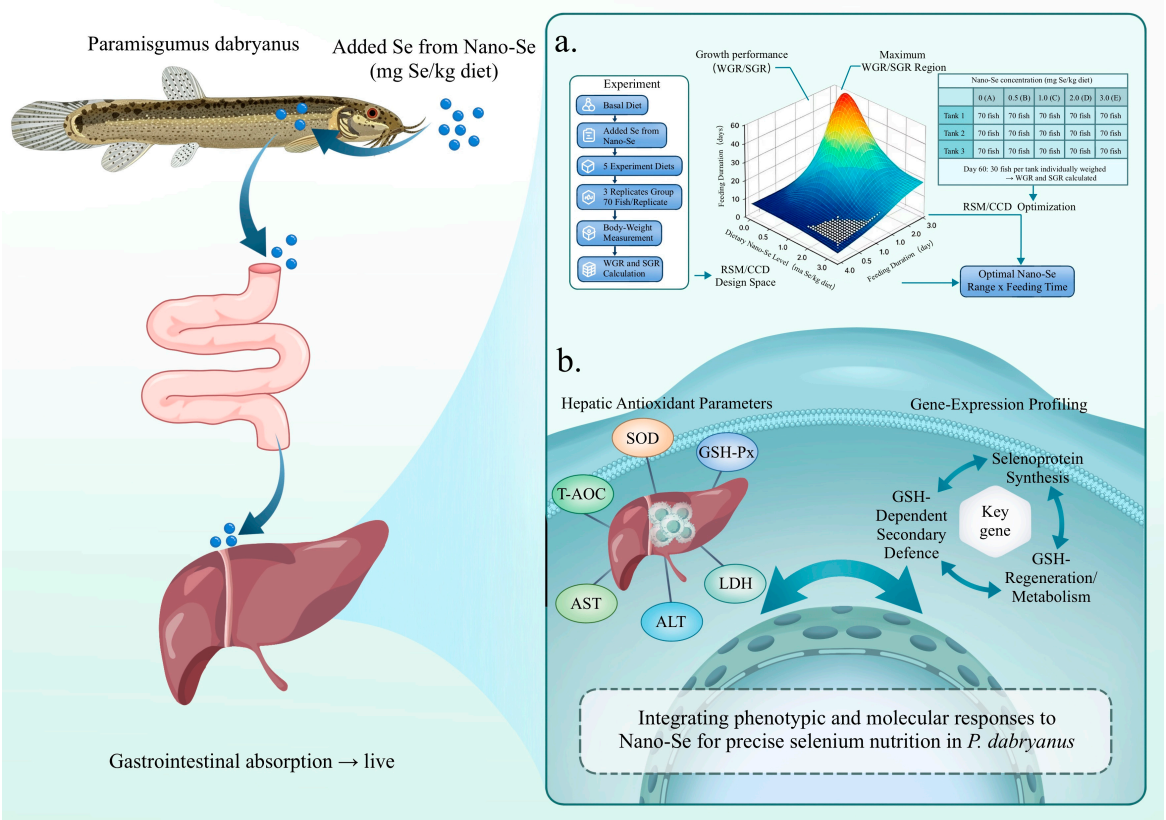


Figure 1. Overview of the experimental design. Note: (**a**) Response surface methodology (RSM/CCD) was used to screen the optimal dietary Nano-Se supplementation level and feeding duration based

on the growth indices (WGR and SGR) of *Paramisgurnus dabryanus*. (**b**) Hepatic antioxidant parameters and the expression of key genes related to selenoprotein synthesis and GSH metabolism were analyzed to characterize the hepatic responses to dietary Nano-Se.

2. Materials and Methods

2.1. Experimental Fish

Juvenile *Paramisgurnus dabryanus* were purchased from a local farm and acclimated in a recirculating aquaculture system at the Jiangxi Fisheries Research Institute for 20 days. During acclimation, water temperature was maintained at 27.0 ± 0.5 °C, dissolved oxygen (DO) ≥ 7.5 mg/L via continuous aeration, and commercial feed was provided twice daily (morning and evening). Before the formal experiment, fish were fasted for 24 h. A total of 1050 healthy juvenile *P. dabryanus* with uniform body size (initial body weight 14.15 ± 1.22 g, mean ± SD) were selected.

2.2. Chemicals and Reagents

Nano-selenium (Nano-Se) was purchased from Yunnan Boshiao Biotechnology Co., Ltd. (Kunming, China). According to the supplier, the product contains 1% selenium, with gelatin as the stabilizing agent. The average particle size is approximately 50 nm, and the zeta potential is approximately 8.3 mV. The commercial kits for total antioxidant capacity (T-AOC), superoxide dismutase (SOD), glutathione peroxidase (GSH-Px), aspartate aminotransferase (AST), alanine aminotransferase (ALT), and lactate dehydrogenase (LDH) were obtained from Nanjing Jiancheng Bioengineering Institute (Nanjing, China). The RNA extraction kit was purchased from Tiangen Biotech (Beijing, China). The HiScript III RT SuperMix for qPCR (+gDNA wiper) kit was obtained from Vazyme (Nanjing, China). The 2× SYBR Green Pro Taq HS premix was purchased from Accurate Biology (Changsha, China). Eugenol was obtained from YSC Flavor Co., Ltd. (Jian, China). All other chemicals and reagents used were of analytical grade and purchased from local suppliers.

2.3. Experimental Design for Growth Performance

The biological effect of Se follows a typical U-shaped curve, with both dietary Se content and feeding duration affecting growth performance. Traditional single-factor experiments cannot reveal the interaction between these two factors. Therefore, response-surface methodology (RSM) was employed to systematically investigate the effects of dietary Nano-Se level and feeding time on growth performance.

2.3.1. Single-Factor Experiments

Single-factor experiments were conducted to analyze the effects of dietary Nano-Se concentration and feeding time on weight-gain rate (WGR) and specific growth rate (SGR), thereby determining the lower and upper bounds of independent variables for the subsequent RSM model.

(1) Nano-Se concentration experiment

Five experimental diets with different Se levels from Nano-Se were formulated. The Nano-Se product contained 1% selenium. It was added to the basal diet to provide 0 (A), 0.5 (B), 1.0 (C), 2.0 (D), and 3.0 (E) mg Se/kg diet. The basal diet composition and nutritional components are shown in Table 1. All ingredients were ground through a 40-mesh sieve, mixed with 15% purified water (*w*/*w*), and pelleted into sinking feed using a pelletizer. Fish were randomly distributed into fiberglass tanks (300 L water volume) with three replicates per group and 70 fish per replicate. The feeding trial lasted 60 days. During the experiment, water temperature was 27.0 ± 0.5 °C, pH 7.5 ± 0.5, and DO ≥ 7.5 ± 0.5 mg/L through 24 h aeration. Daily feeding rate was 3–5% of body weight, adjusted weekly

according to feed intake. Water-quality parameters (temperature, DO, pH) were monitored weekly and remained stable throughout the trial. In addition, fish behavior and feeding responses were observed daily to ensure environmental stability. Body weight was measured on day 60, and WGR and SGR were calculated, 30 fish were randomly selected from each tank and individually weighed. The concentration range where maximum WGR and SGR occurred was selected for the RSM design.

$$\text{Weight-gain rate (WGR, \%)} = (Wt - W0)/W0 \times 100\%$$

$$\text{Specific growth rate (SGR, \%·d}^{-1}\text{)} = (\ln Wt - \ln W0)/\text{rearing days} \times 100\%$$

where W0 is initial body weight (g) and Wt is final body weight (g).

Data were processed using Excel 2019 and SPSS 27.0. One-way ANOVA was performed, and differences were considered significant at $p < 0.05$.

Table 1. Experimental basic-feed formula and nutritional components.

Ingredients (%)	A	B	C	D	E
Fish meal	20.00	20.00	20.00	20.00	20.00
Soybean meal	18.00	18.00	18.00	18.00	18.00
Vegetable meal	10.00	10.00	10.00	10.00	10.00
Chicken meal	5.00	5.00	5.00	5.00	5.00
Fermented soybean meal	10.00	10.00	10.00	10.00	10.00
Corn-protein flour	10.00	10.00	10.00	10.00	10.00
Bean oil	4.00	4.00	4.00	4.00	4.00
Corn starch	16.00	16.00	16.00	16.00	16.00
Yeast hydrolysate	2.00	2.00	2.00	2.00	2.00
CaH2PO4	2.00	2.00	2.00	2.00	2.00
Choline chloride	0.50	0.50	0.50	0.50	0.50
Vitamin premix and mineral premix [1]	1.00	1.00	1.00	1.00	1.00
Sodium alginate	1.50	1.50	1.50	1.50	1.50
Total	100.00	100.00	100.00	100.00	100.00
Added Se from Nano-Se (mg Se/kg diet)	0.00	0.50	1.00	2.00	3.00
Measured total selenium content (mg/kg)	1.42	1.9	2.35	3.31	4.27

[1] The Vitamin premix and mineral premix the following per kg of diets: VA 16,000 IU, VD 33,000 IU, VC 200 mg, VE 200 mg, VK 320 mg, VB1 13.4 mg, VB2 20 mg, VB6 30 mg, VB12 27 mg, D-calcium pantothenate acid 80 mg, nicotinic acid 130 mg, folic acid 6.6 mg, biotin 1000 mg, Inositol 270 mg, Ca $(H_2PO_4)_2 \cdot H_2O$ 400 mg, calcium lactate 1000 mg, Fe (as ferric citrate) 100 mg, Mg (as magnesium sulfate) 400 mg, Al (as aluminum chloride) 20 mg, Zn (as zinc chloride) 60 mg, Cu (as copper sulfate) 30 mg, Mn (as manganese sulfate) 20 mg, Potassium iodide 20 mg. The negative control diet (Group A) contained no added Nano-Se; its Se content (1.42 mg/kg) originated from the natural background of feed ingredients (fish meal and soybean meal), as the vitamin/mineral premix contained no added Se.

(2) Feeding duration experiment

Fish were fed the optimal Nano-Se concentration determined above (1.0 mg/kg). Body weight was measured on days 0, 20, 30, 40, 50, and 60, and WGR and SGR were calculated. The time range where maximum values occurred was selected for the RSM design. Statistical methods were the same as above.

2.3.2. Response-Surface Methodology Optimization

Based on the results of 2.3.1, a central-composite design (CCD) with two factors and five levels was used. Although the single-factor experiment preliminarily identified 1.0

mg Se/kg diet as the optimal Se level from Nano-Se, the U-shaped dose-response of Se necessitates inclusion of both deficiency (0 mg/kg) and excess (>3.0 mg/kg) ranges. To accurately fit the non-linear relationship across the full response domain (including both limbs around the turning point), the factor range was set from 0 to 4 mg Se/kg diet, covering deficient, optimal, and excessive levels to avoid boundary extrapolation. The two factors were dietary Nano-Se concentration (T) and feeding duration (S), and the response variables were WGR and SGR. The experimental factors and levels are shown in Supplementary Table S1. A quadratic polynomial regression equation was fitted using the least-squares method in Design-Expert 8.0:

$$Y = b_0 + b_1T + b_2S + b_3TS + b_4T^2 + b_5S^2$$

where Y is the predicted value of WGR or SGR; b_0 is the intercept; b_1 and b_2 are linear coefficients; b_3 is the interaction coefficient; b_4 and b_5 are quadratic coefficients. The significance level was set at $\alpha = 0.05$. Rearing conditions were the same as in the single-factor experiments.

2.4. Biochemical Index Measurement

To evaluate the effects of Nano-Se on antioxidant and metabolic performance of *P. dabryanus*, fish were fed the five experimental diets (Groups A–E) as described in 2.3.1. Sampling was performed on days 0, 20, 40, and 60. Four fish per group were sampled for biochemical and gene-expression analyses, based on previous fish-selenium-nutrition studies (3–6 biological replicates) [14–16] and the 3R principle for ethical animal use [17]. Liver tissues were collected, immediately frozen in liquid nitrogen, and stored at −80 °C. T-AOC, SOD, GSH-Px, AST, ALT, and LDH were measured using commercial kits following the manufacturer's instructions.

Data are presented as mean ± standard deviation. One-way ANOVA followed by Duncan's multiple range test was performed using Excel 2019 and SPSS 27.0, with $p < 0.05$ considered significant. Heatmap and correlation analyses are described in Section 2.6.

2.5. Gene Expression Analysis of Key Selenium Metabolism Genes

Dietary Nano-Se gradients and sampling were the same as in 2.4. Total RNA was extracted from liver using an RNA extraction kit. RNA concentration and purity were measured with a Nanodrop 2000 (Thermo Fisher Scientific, Waltham, MA, USA), and integrity was assessed by agarose gel electrophoresis. cDNA was synthesized using the HiScript III RT SuperMix for qPCR (+gDNA wiper) kit. Primers were designed using Premier 5.0 and are listed in Table 2. To ensure reliable normalization, three candidate reference genes (*ef1α*, *β-actin*, and *gapdh*) were evaluated for expression stability using geNorm analysis. The M-values for *ef1α* and *β-actin* were 0.489 and 0.497, respectively (both below the 0.5 threshold), while *gapdh* showed a higher M-value of 0.596 and was therefore excluded. The amplification efficiencies of *ef1α*, *β-actin*, and *gapdh* were 100.17%, 97.70%, and 83.09%, respectively; *ef1α* and *β-actin* fell within the acceptable range (90–110%), whereas *gapdh* did not meet this criterion. The M-value and efficiency data for all candidate genes are provided in Table S2, Figures S1 and S2 (Supplementary Materials). Consequently, *ef1α* and *β-actin* were selected as the reference genes for subsequent normalization. Relative expression levels were calculated according to Hellemans and Vandesompele [18]. All primers showed satisfactory amplification performance, with efficiency values ranging from 94.3% to 107.7%. qPCR was performed on a StepOne Plus Real-Time PCR System (Thermo Fisher, USA). The 20 μL reaction mixture contained: 10 μL 2× SYBR Green Pro Taq HS premix, 0.8 μL each of forward and reverse primer (10 μmol/L), 2 μL cDNA, and 6.4 μL DEPC-treated water. The thermal cycling protocol was: 50 °C for 2 min; 95 °C for

30 s; 40 cycles of 95 °C for 15 s and 58 °C for 45 s; followed by 95 °C for 15 s and 72 °C for 5 min.

Relative gene expression was calculated using the 2−ΔΔCt method and presented as mean ± standard deviation. GraphPad Prism 8 was used for graphing, and one-way ANOVA followed by Duncan's test ($p < 0.05$) were performed with SPSS 27.0. Heatmap and correlation analyses are described in Section 2.6.

Table 2. Sequences of primers used for qRT-PCR.

Genes	Primer Sequence	Accession Number	Product Length (bp)	Amplification Efficiency (%)
selenoo1	F: AGACAAGAGCACGTTGGTCC R:GCCAGCCGCTGTCTGTATTT	XM_065278813.2	138	108.14
trnau1ap	F: CCTCCTCCAGTTCCACAAGG R: TTTGGATCTTCGGCAGGGTC	XM_065276277.1	131	96.57
selenop2	F:TTGACCTTCCATATTGTACTGCC R:TGCCGACTATTGTCTCCTGTG	XM_065276391.2	123	92.42
gpx1	F: ACACCCGCTTTGGGAATCAA R:CGGACATATTTCAGAGAAAGGAGG	XM_065240964.2	112	104.04
chac2	F: AATTACCTTGGCCCAGCTCC R: ATTTTTGCCACTGGGGCCTA	XM_065242312.2	75	92.24
hagh	F: CCCAGAAGGTTGTGGATGCT R: AGTGATGGTGCGTGGTAAGG	XM_065252947.2	72	92.34
glo1	F:CAATGGCAACTCAGATCCACG R:GGTCACTCCCTGCTCCTCAAA	XM_065296127.1	97	96.06
mgstt2	F:CACTGGCAGAACTGGAGGAG R: GGCTGCATGAGCTCACAAAC	XM_065250952.2	124	93.81
mgst3b	F:TGCCAGGAAGAAGTTTGGCA R: TCCAGTGTGTTCTGATGGGC	XM_065296140.2	96	104.76
selenop	F: GATGTCTGGCAGGCGGTAA R:CTCAGGACGGTGTAGGGAAGT	XM_065247254.1	101	101.56
gsr	F:GATGAAAAGGTGGTTGGTCTCC R:TGTAGGGTGTATGGCAATGGTT	XM_065273062.2	129	103.67
selenot1a	F:TACCCAGACATCCGCATAGAA R:CTTGCCCACAATAATCACTCCT	XM_065269807.2	117	94.69
ef1α	F: ACAGCAAGAACGACCCACC R: AAAGCGACCAAGAGGAGGAT	XM_065290951.1	290	100.17
β-actin	F: TCTTGGGTATGGAGTCTTGCGGT R: TCTTGATTTTCATTGTGCTGGGG	XM_065254272.1	113	97.70
gapdh	F:TGTCTTCTGTGTGGCAGTGTAAGC R:GCTCCCCTGGCTAAAGTCATTCATG	XM_065298779.1	101.2	83.09

2.6. Heatmap and Correlation Analysis

Heatmap analysis: To eliminate dimensional differences and initial individual variation, the biochemical indices and gene-expression data were analyzed separately. Within each dataset, all data were transformed to $\log_2$ fold change ($\log_2$FC) relative to day 0 within the same Nano-Se concentration group, calculated as $\log_2$ (treatment mean/day 0 mean of the same Nano-Se concentration). This transformation was used because (1) different indicators within the same dataset have different units and scales, and $\log_2$FC eliminates these dimensional differences, allowing a common color scale in the heatmap; (2) using each group's own day 0 as baseline reduces the influence of initial individual variation; and (3) this transformation focuses on the temporal dynamics of each indicator.

Hierarchical clustering (Euclidean distance, complete linkage) was performed on log_2FC matrices of biochemical indices and gene expression data separately using the R package heatmap. Clustering was applied to both indicators (rows) and time-concentration combinations (columns). Red and green color scales indicate positive (up-regulation) and negative (down-regulation) log_2FC values.

Correlation analysis: Global correlations were assessed using Spearman correlation, which captures monotonic relationships without assuming linearity or normality. Stratified analyses used Pearson correlation for linear relationships. Scatter plots were visually inspected for obvious non-linear patterns. Data from five Nano-Se concentration groups (A–E) at three time points (20, 40, 60 d) were analyzed as 15 treatment–time combinations to explore potential associations among biochemical indices and gene expression. We acknowledge that measurements from the same concentration group at different time points may not be fully independent; therefore, this analysis was considered exploratory, and stratified analyses by concentration and by time were also performed; these stratified analyses do not rely on the assumption of independence across all 15 combinations. The significance level was $\alpha = 0.05$. Statistical analyses were performed using SPSS 27.0, and heatmaps were generated with the R package heatmap.

3. Results

3.1. Single-Factor Experiment Results

3.1.1. Effect of Nano-Se Concentration on Growth Performance

After 60 days of feeding with Nano-Se diets, the effects of different Nano-Se concentrations on growth performance of *P. dabryanus* are shown in Figure 2. As the Se from Nano-Se addition increased from 0 to 3.0 mg Se/kg diet, both weight-gain rate (WGR) and specific growth rate (SGR) first increased and then decreased. The maximum WGR and SGR were observed at 1.0 mg Se/kg diet, while the minimum occurred at 3.0 mg/kg. Thus, under single-factor conditions, the optimal Se concentration for both WGR and SGR was 1.0 mg/kg.

3.1.2. Effect of Feeding Duration on Growth Performance

Using the optimal Nano-Se concentration (1.0 mg Se/kg diet), the effects of feeding duration on growth performance are shown in Figure 3. WGR increased continuously with time, reaching a maximum at 60 d and minimum at 20 d. SGR peaked at 30 d and then slightly declined, with no significant differences among groups after 30 d ($p > 0.05$). Therefore, the optimal feeding duration for WGR was 60 d, and for SGR was 30 d under single-factor conditions.

3.2. Response-Surface Methodology for Growth-Performance Optimization

3.2.1. WGR Model Building and Response-Surface Analysis

The central-composite design (CCD) results are presented in Supplementary Table S3. After coding (as shown in Supplementary Table S1), multiple regression was performed to obtain the quadratic regression Equation (1) for WGR (Y): $Y = 6.373 + 58.719\ T + 0.232\ S - 0.290\ TS - 17.649\ T^2 + 0.022\ S^2$, where Y is WGR (%), T is coded Se level from Nano-Se (mg Se/kg diet), and S is coded feeding duration. Based on the regression coefficients and their significance levels, the relative contribution of each factor to the response was evaluated.

ANOVA results for the WGR model are shown in Supplementary Table S4. The model was highly significant ($F = 82.79$, $p < 0.001$), and the lack-of-fit was not significant ($p = 0.0658 > 0.05$). $R^2 = 0.9834$, adjusted $R^2 = 0.972$, indicating that the model explains 97.2% of the response variation. AP = 29.479 > 4, CV = 6.59% < 10%, confirming model reliability.

The linear terms T (Se level from Nano-Se) and S (time) were both highly significant ($p < 0.01$), the quadratic term T^2 was significant ($p < 0.01$), while S^2 ($p = 0.3066$) and the interaction TS ($p = 0.0988$) were not significant. The order of influence on WGR was S > T.

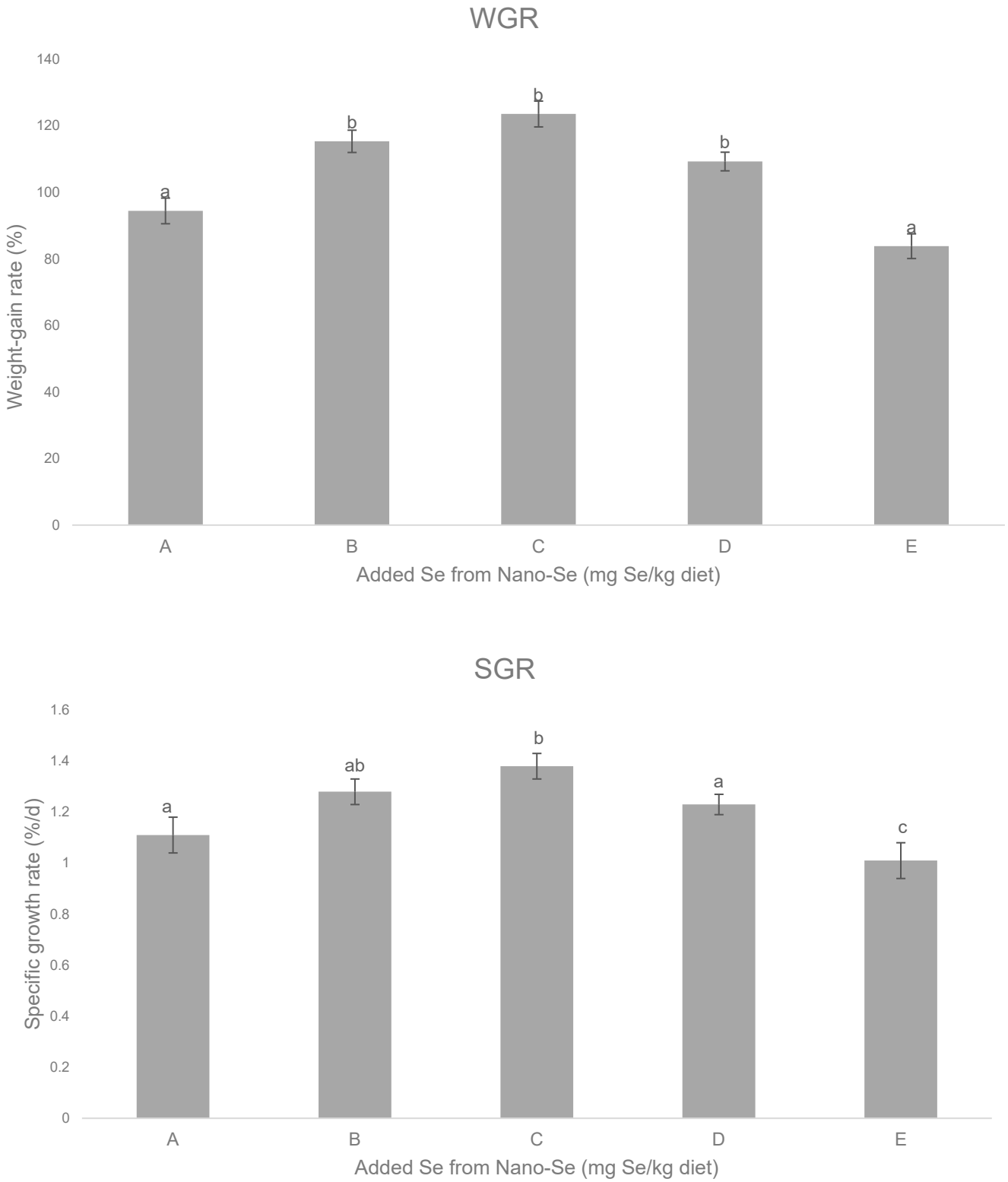
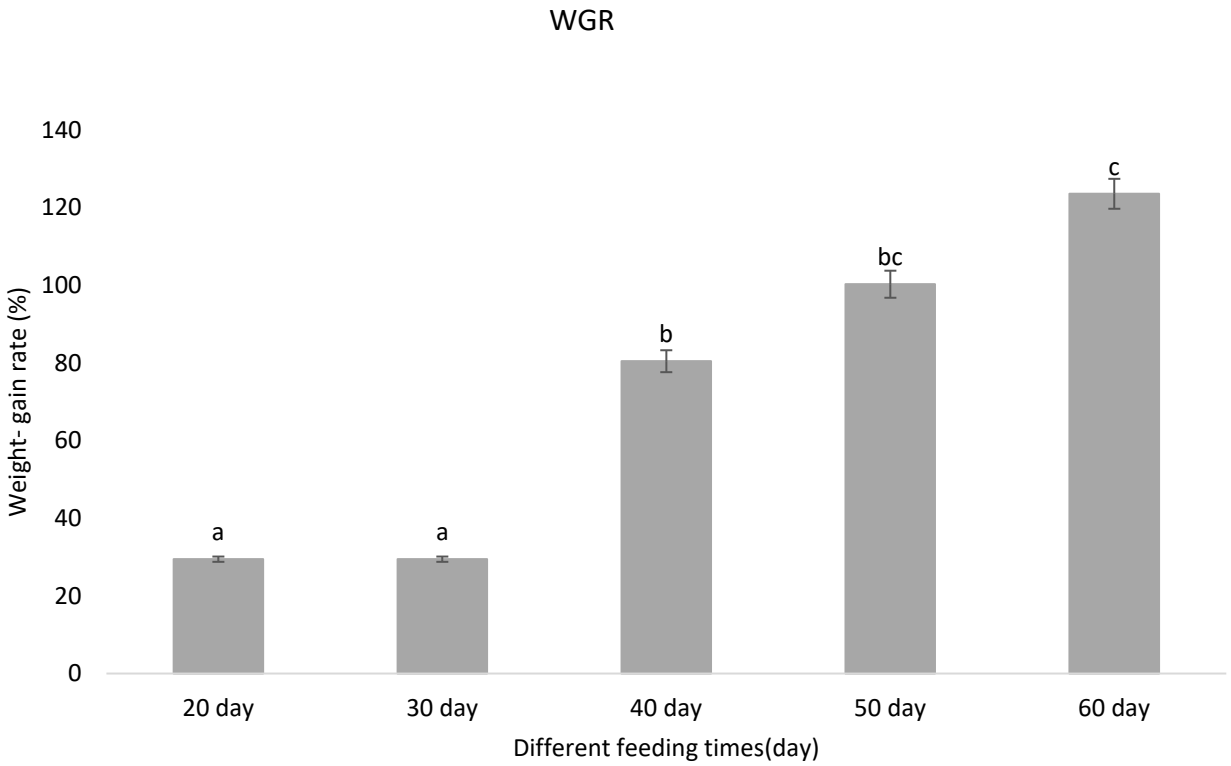
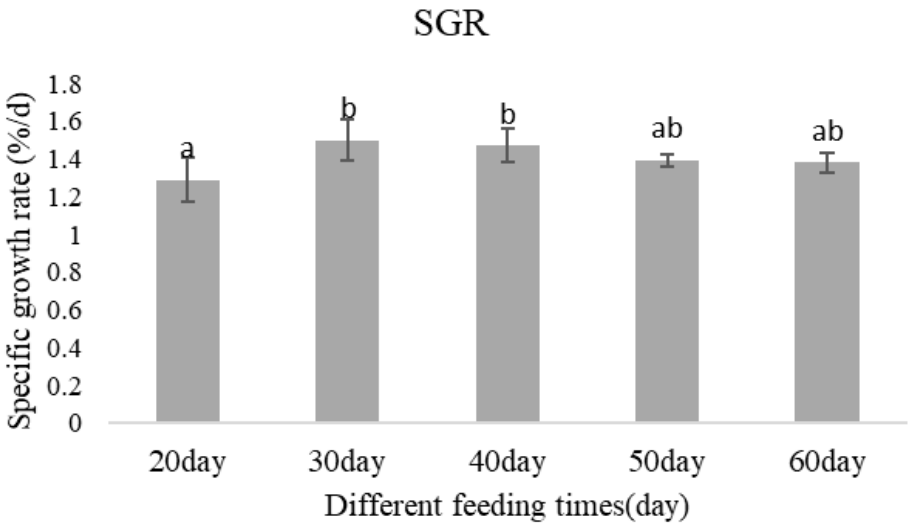


Figure 2. Effect of different Se levels from Nano-Se on growth performance. WGR, weight-gain rate (%); SGR, specific growth rate (%/d). Data are presented as mean ± SD (n = 3 replicate tanks per group, 30 fish per tank). Different letters indicate significant differences among groups ($p < 0.05$).





https://doi.org/10.3390/antiox15111392

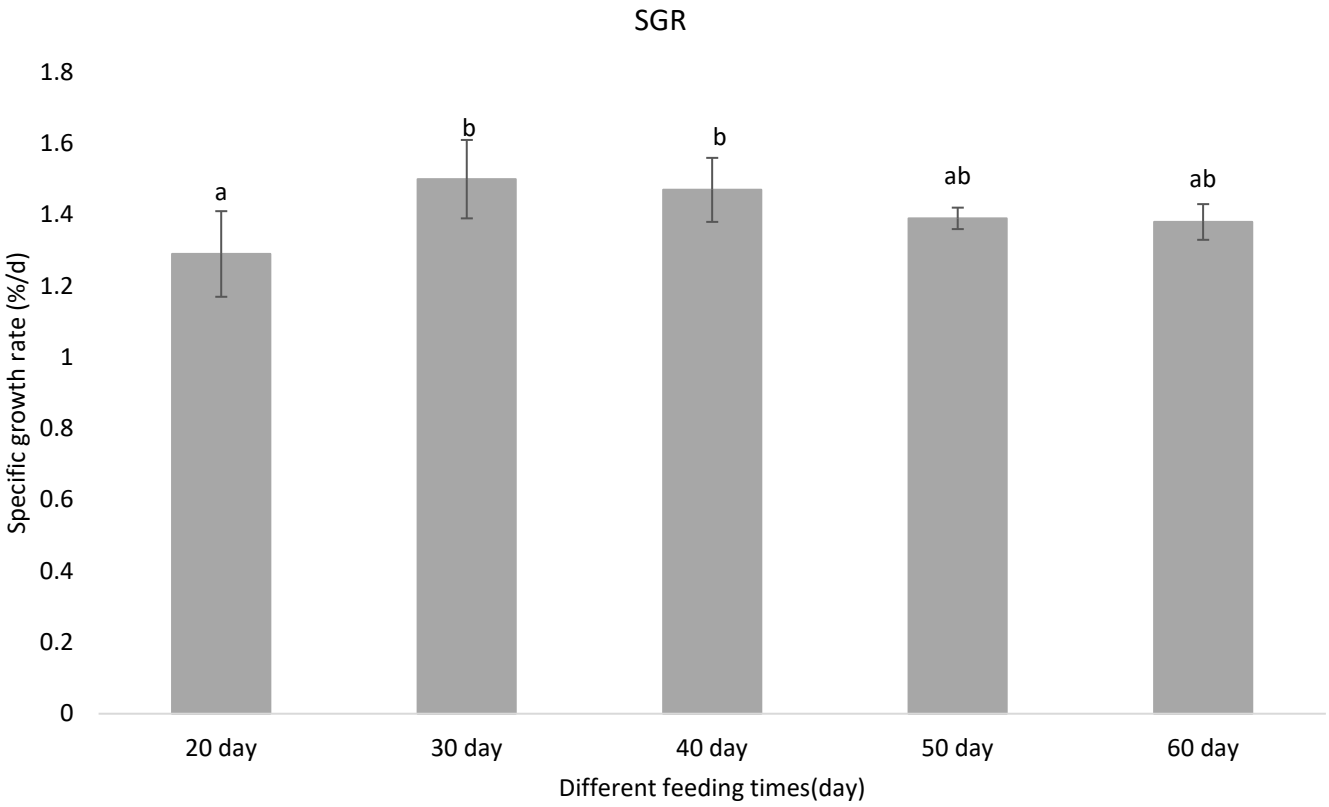


Figure 3. Effect of feeding duration on growth performance at 1.0 mg Se/kg diet from Nano-Se. WGR, weight-gain rate (%); SGR, specific growth rate (%/d). Data are presented as mean ± SD (n = 3 replicate tanks per group, 30 fish per tank). Different letters indicate significant differences among groups ($p < 0.05$).

3.2.2. SGR Model Building and Response-Surface Analysis

The SGR response-surface results are shown in Supplementary Table S5. The quadratic regression Equation (2) for SGR (Y) after coding was: $Y = 0.639 + 0.493\ T + 0.027\ S - 0.001\ TS - 0.167\ T^2 - 0.0003\ S^2$. ANOVA (Supplementary Table S6) showed that the model was significant ($F = 15.18$, $p = 0.0012$), with a non-significant lack-of-fit ($p = 0.0583$). $R^2 = 0.9156$, adjusted $R^2 = 0.8552$, AP = 11.1484 > 4, CV = 4.99% < 10%. The linear term T (Nano-Se) and quadratic term T^2 were highly significant ($p < 0.01$), while S (time) was not significant ($p = 0.8064$), S^2 approached significance ($p = 0.0579$), and TS was not significant ($p = 0.7305$). The influence order was T > S.

3.2.3. Interactive Effects of Nano-Se Concentration and Feeding Duration on WGR and SGR

Response surface and contour plots (Figures 4 and 5) were generated from Equations (1) and (2). Figure 4 shows that WGR first increased and then decreased with increasing Nano-Se concentration, peaking at about 1.0 mg/kg; at the same concentration, WGR continuously increased with feeding duration, reaching a maximum at 60 d. Figure 5 shows that SGR also exhibited a parabolic response to Nano-Se concentration, with the optimum at ~1.0 mg/kg; however, with prolonged feeding, SGR first increased and then decreased, peaking at 30 d. The upward-convex surfaces indicate the existence of maximum values. Numerical optimization using Design-Expert 8.0 predicted the optimal conditions for maximum WGR as 1.171 mg/kg Nano-Se and 60 days (predicted WGR = 121.934%), and

for maximum SGR as 1.395 mg/kg Nano-Se and 39.75 days (predicted SGR = 1.512%/d). These predicted optima are consistent with the experimental observations.

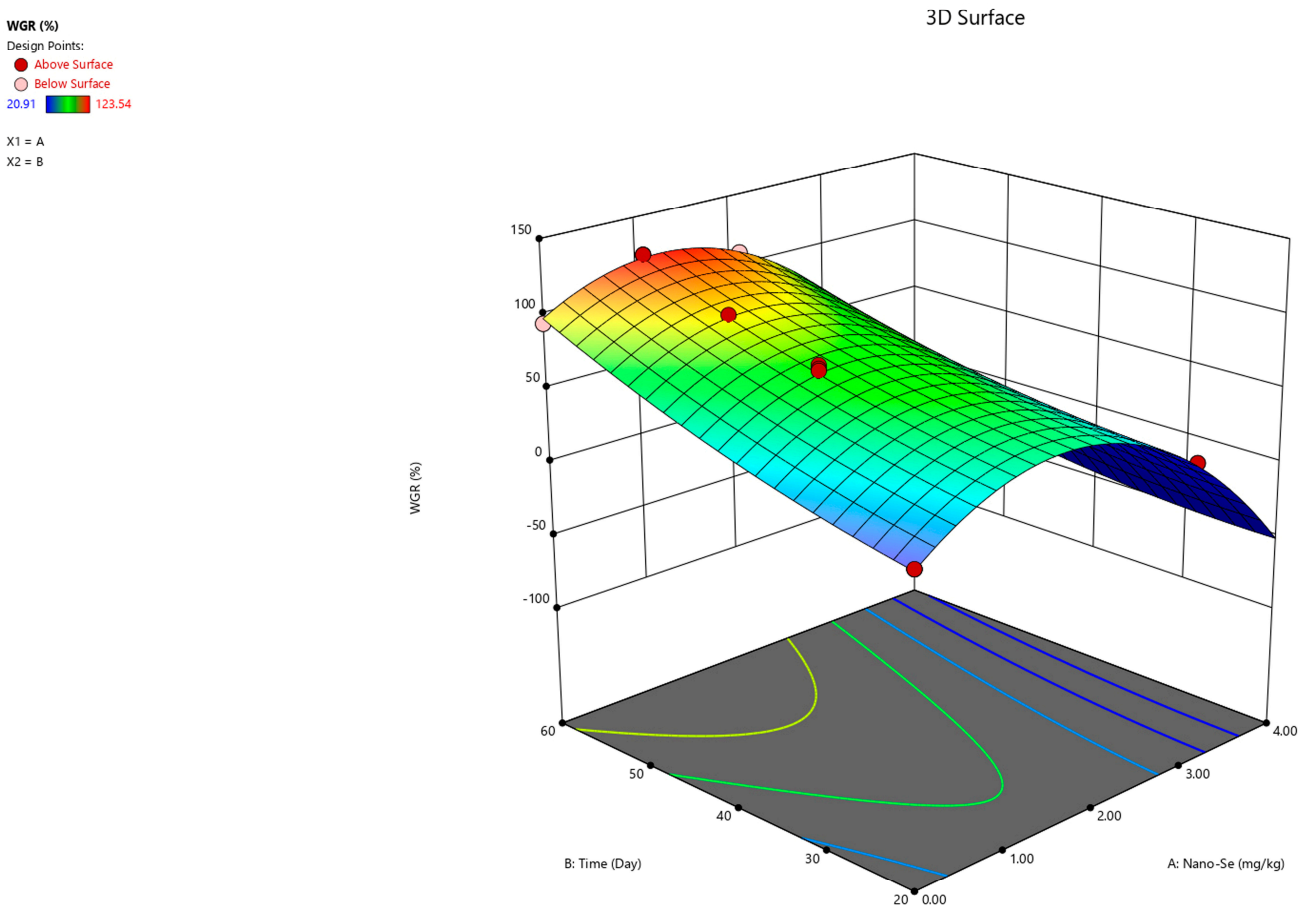


Figure 4. Response-surface plot (3D) and contour plot showing the interactive effects of Nano-Se concentration and feeding duration on WGR. The color scale represents the predicted WGR values, with warmer colors indicating higher WGR and cooler colors indicating lower WGR. Contour lines connect points of equal predicted WGR. Red circles represent the experimental design points.

3.3. Dynamic Changes and Heatmap Clustering of Hepatic Biochemical Indices

3.3.1. Time and Dose Effects on Enzyme Activities

As shown in Figure 6, in the control group (Group A, 0 mg Se/kg diet), liver T-AOC, SOD, GSH-Px, LDH, AST, and ALT activities generally increased first and then decreased, or continuously increased, peaking or remaining high at 40–60 d. Compared to the control, low-dose Nano-Se (Group B, 0.5 mg Se/kg diet) significantly inhibited SOD and GSH-Px activities. The medium dose (Group C, 1.0 mg Se/kg diet) maintained stable antioxidant capacity during the mid-culture period, with a smaller decline in transaminases at later stages. High doses (Groups D, 2.0 mg Se/kg diet; E, 3.0 mg Se/kg diet) strongly activated GSH-Px and SOD but caused significant reductions in AST and ALT activities after prolonged feeding (60 d).

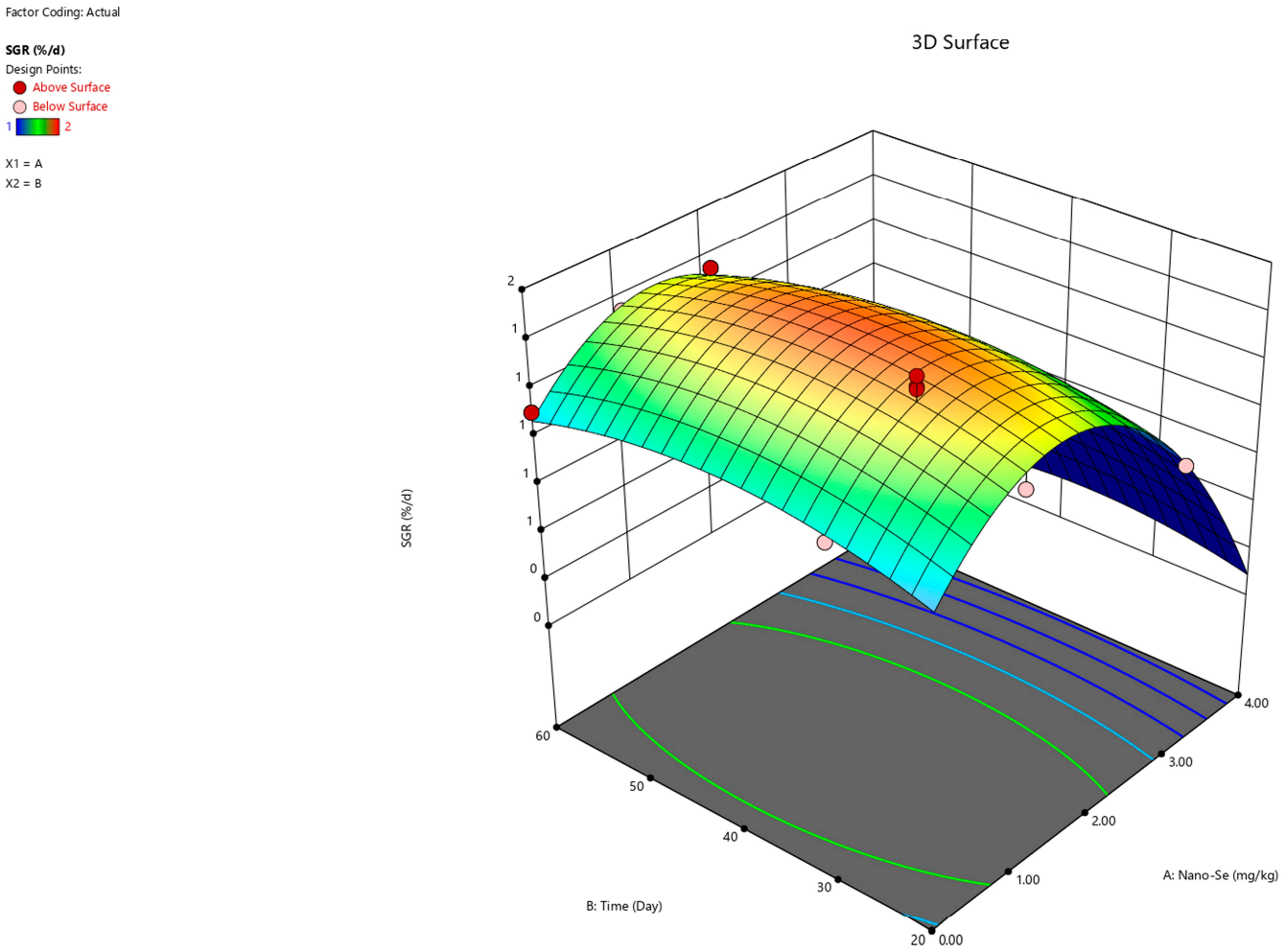
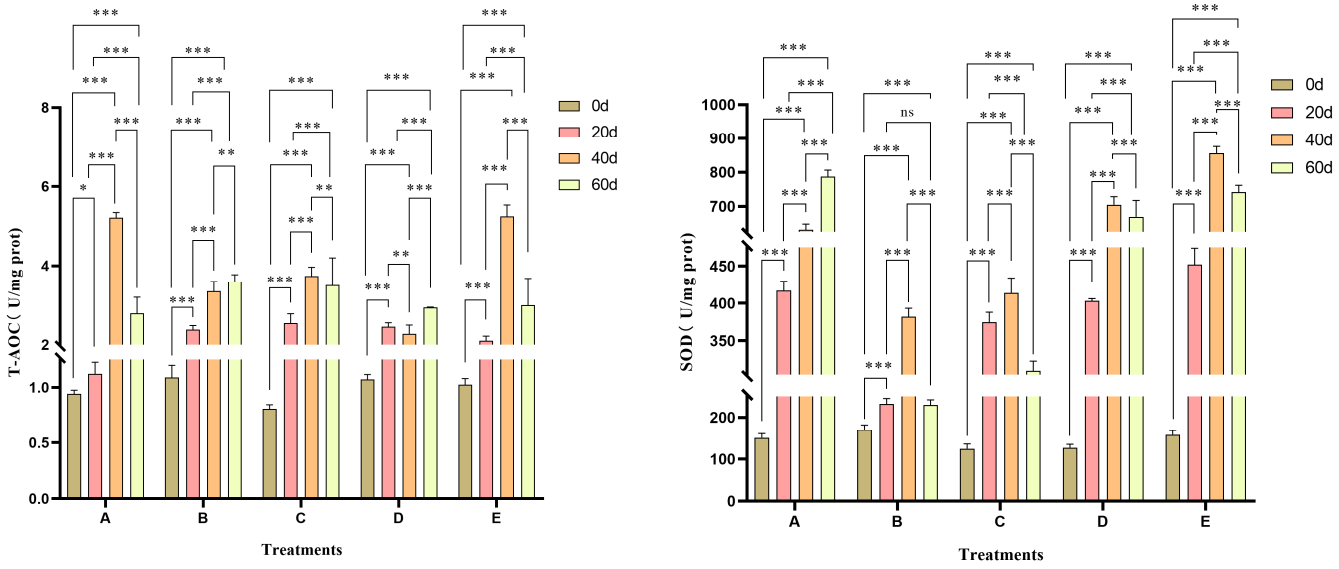


Figure 5. Response-surface plot (3D) and contour plot showing the interactive effects of Nano-Se concentration and feeding duration on SGR. The color scale represents the predicted SGR values, with warmer colors indicating higher SGR and cooler colors indicating lower SGR. Contour lines connect points of equal predicted SGR. Red circles represent the experimental design points.



https://doi.org/10.3390/antiox15111392

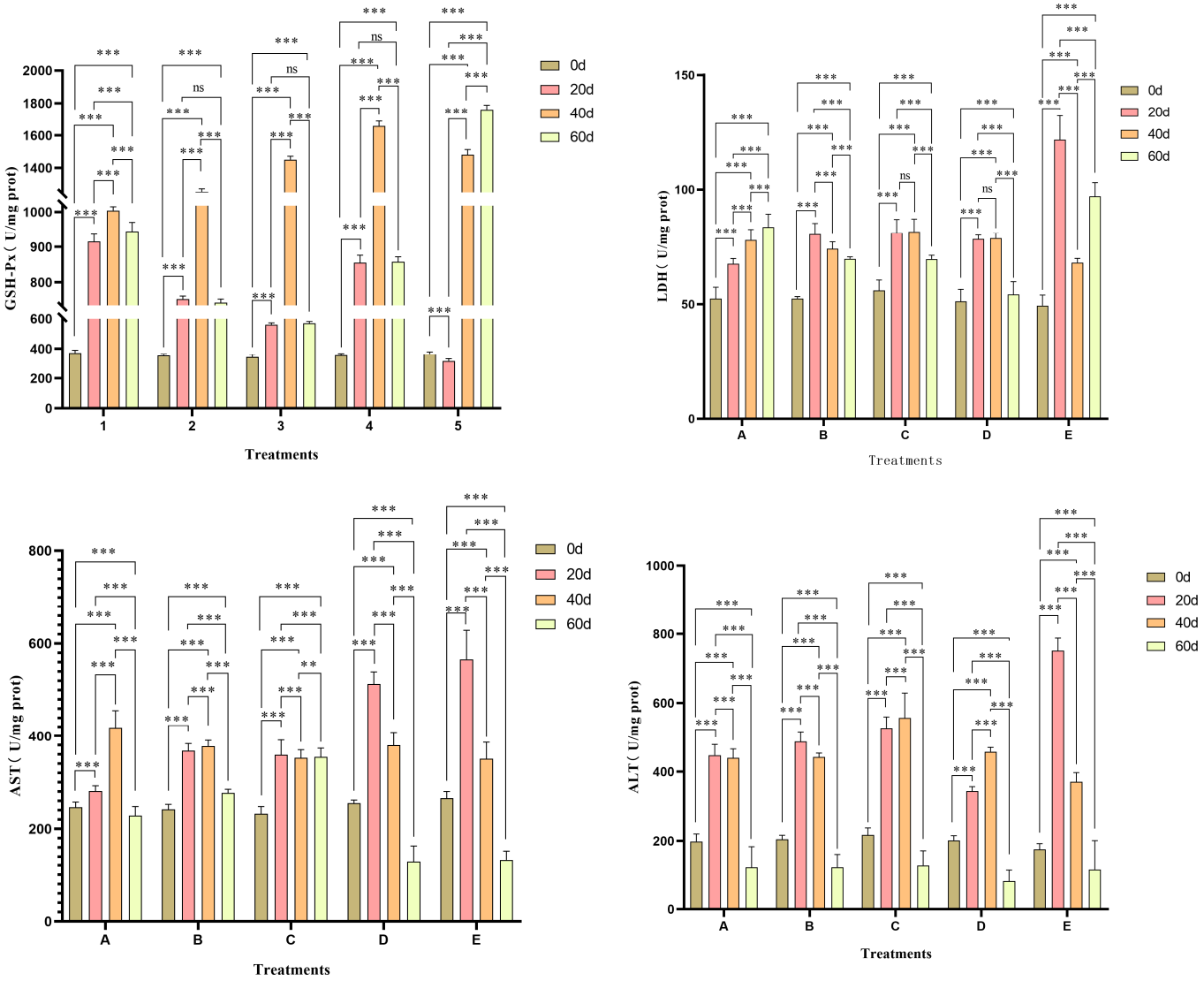


Figure 6. Changes in liver biochemical indices under different Se levels from Nano-Se and feeding durations. Asterisks indicate levels of significance (ANOVA with post hoc Tukey test, * $p < 0.05$; ** $p < 0.01$; *** $p < 0.001$, ns stands for not significant).

3.3.2. Heatmap-Clustering Analysis of Hepatic Biochemical Indices

Hierarchical clustering heatmaps were constructed based on log_2FC relative to day 0 (Figure 7). Indicator clustering: ALT and AST clustered together (transaminases); T-AOC and GSH-Px clustered together (antioxidant system); SOD and LDH clustered together (linking oxidative stress and energy metabolism). Treatment clustering: A20, A40, E20, E40, D20 formed a cluster with all indicators up-regulated (red), indicating general metabolic activation. C60, D40, C20, D60, C40 formed a cluster with all indicators down-regulated (green), suggesting metabolic inhibition by medium/high Nano-Se in the middle-late period. B20, B40, B60 formed a cluster with up-regulated transaminases but down-regulated antioxidant enzymes, indicating that low dose maintains amino acid metabolism but weakens antioxidant defense. A60 and E60 formed a cluster with down-regulated transaminases (green) while T-AOC, SOD, GSH-Px remained strongly up-regulated (red), showing an "uncoupling" phenomenon.

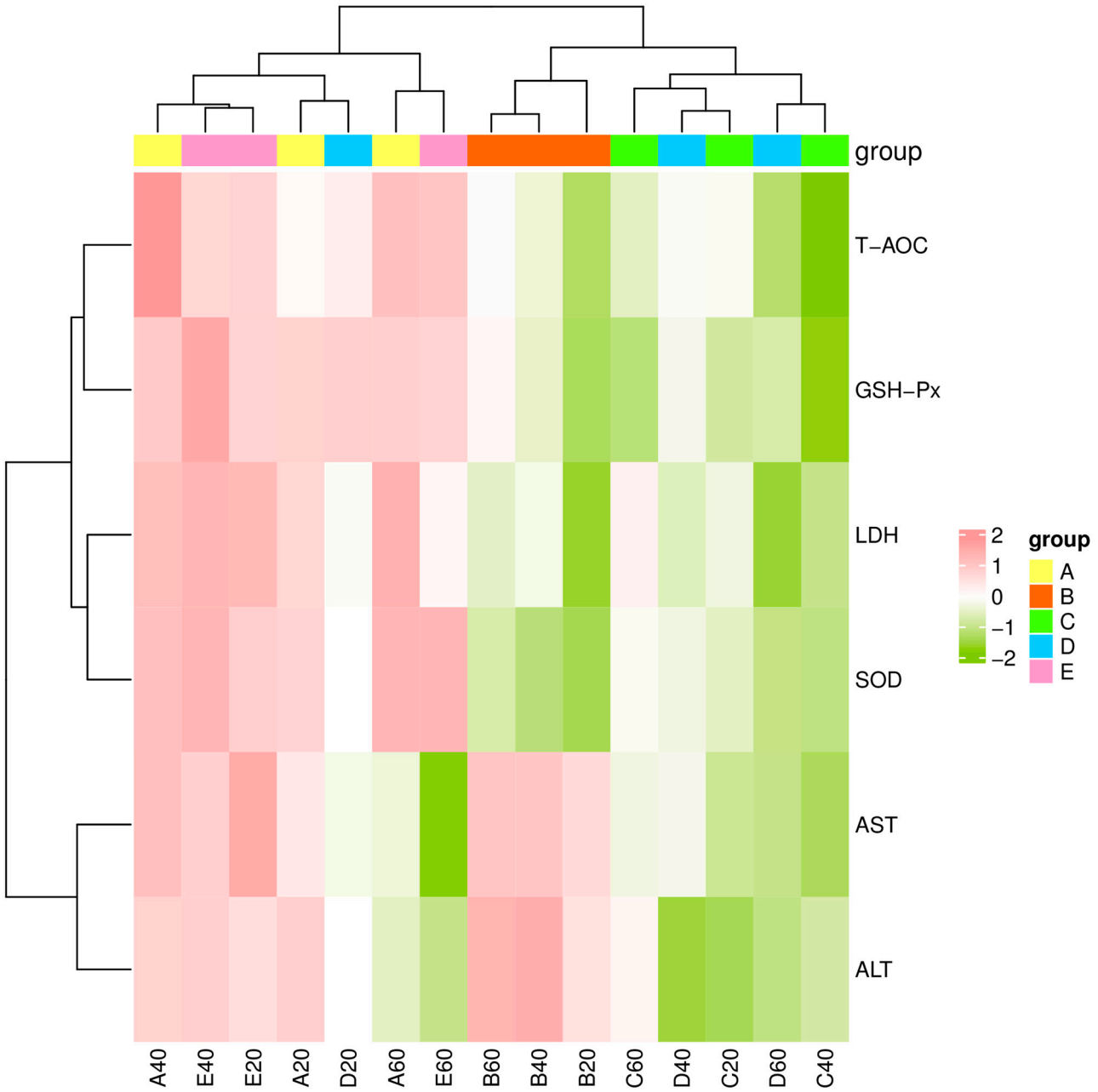


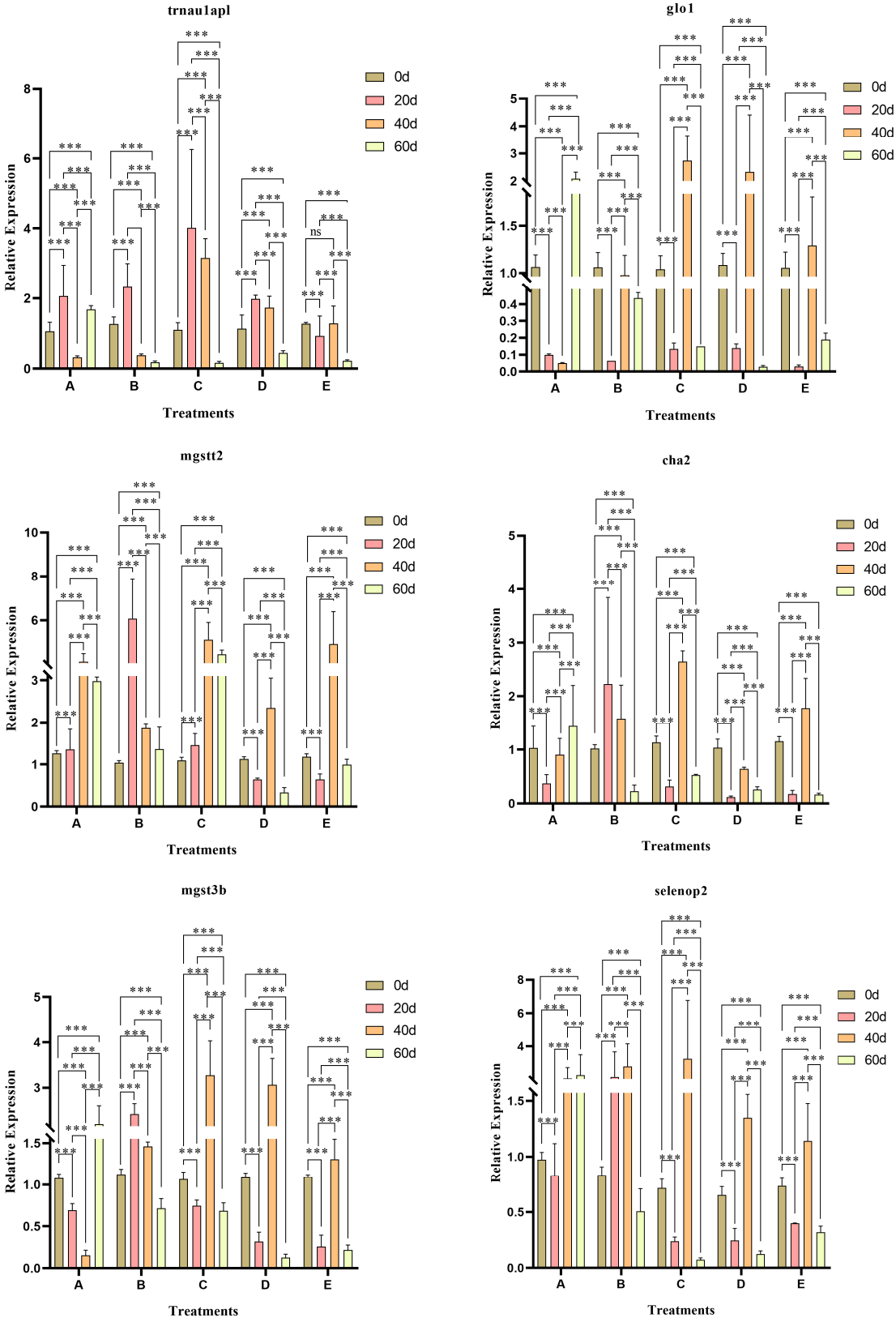
Figure 7. Heatmap clustering of $\log_2$ fold change ($\log_2$FC) of hepatic biochemical indices. Rows: indicators; columns: time-concentration combinations. Red, up-regulation; green, down-regulation.

3.4. Dynamic Changes and Heatmap Clustering of Hepatic Selenium Metabolism-Related Gene Expression

3.4.1. Gene-Expression Dynamics

As shown in Figure 8, Selenoprotein genes (selenoprotein O1 (*selenoo1*), selenoprotein T1a (*selenot1a*)) were continuously highly expressed in the control group at mid-late stages, while in Nano-Se-supplemented groups they peaked at 40 d and then sharply decreased. Glutathione metabolism-related genes (microsomal glutathione S-transferase 3b (*mgst3b*), microsomal glutathione S-transferase 2 (*mgstt2*), ChaC glutathione-specific gamma-glutamylcyclo transferase 2 (*chac2*), hydroxyacyl glutathione hydrolase (*hagh*), glyoxalase I (*glo1*), glutathione reductase (*gsr*), glutathione peroxidase 1 (*gpx1*)) generally peaked at 40 d in Group C (1.0 mg Se/kg diet), but at 60 d most supplemented groups had lower expression than the control. Genes such as tRNA selenocysteine 1 associated protein

(*trnau1ap*, *selenop*), and selenoprotein P2 (*selenop2*) were significantly suppressed in supplemented groups at later stages, especially in high-dose groups (D, E) at 60 d.



https://doi.org/10.3390/antiox15111392

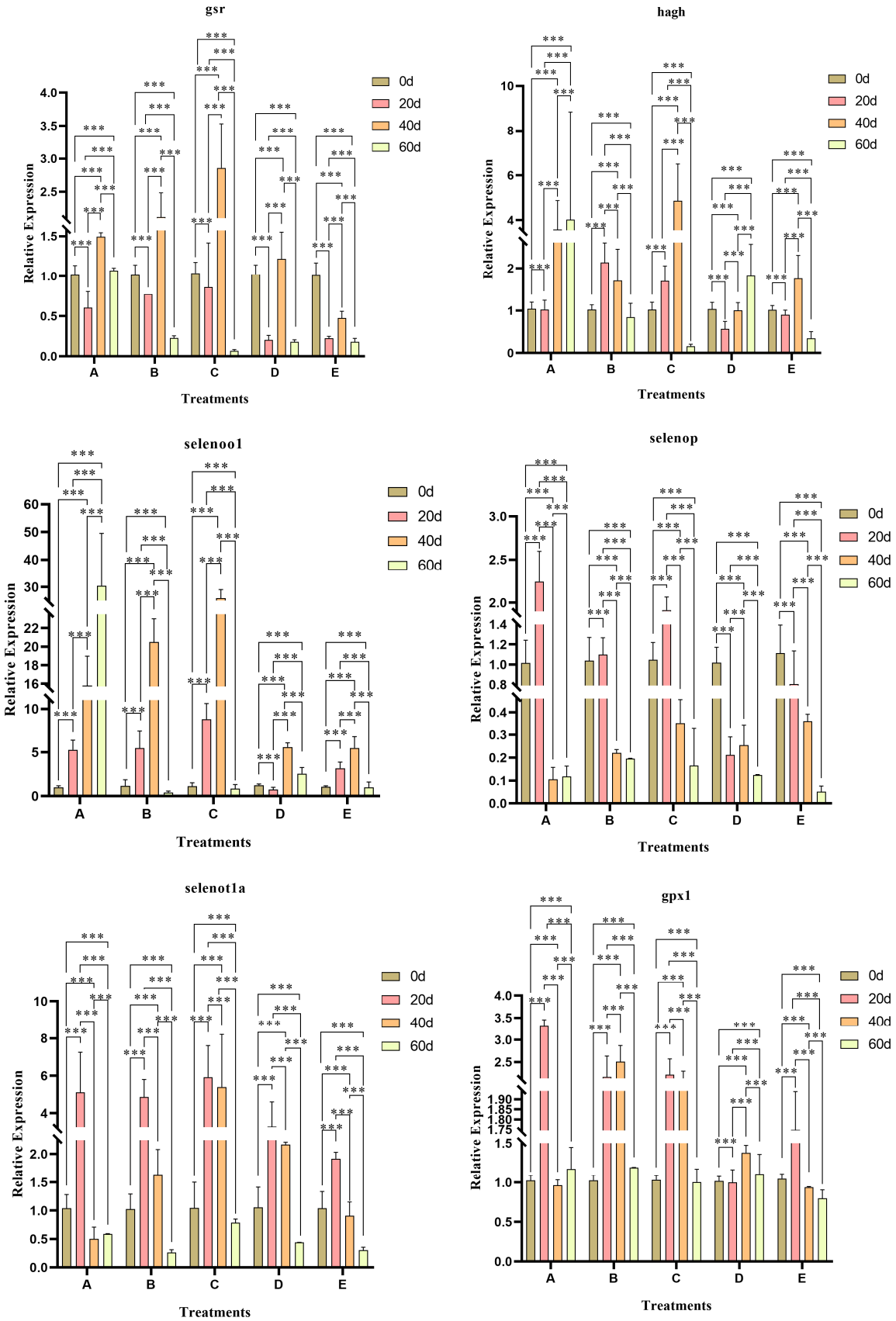


Figure 8. Expression dynamics of selected selenium metabolism-related genes in liver under different Nano-Se doses and feeding durations. Asterisks indicate levels of significance (ANOVA with post hoc Tukey test, *** $p < 0.001$, ns stands for not significant.).

3.4.2. Heatmap-Clustering Analysis of Selenium Metabolism-Related Gene Expression

The heatmap of log_2FC for gene expression (Figure 9) separated the 12 functional genes into three clusters. Cluster I (*selenop*, *selenot1a*, *gpx1*, *trnau1ap*): selenoprotein synthesis-related genes, showing a pattern of "early sustained high expression, late gradual decline". At 60 d, all supplemented groups exhibited suppression, and the degree of suppression increased with Se concentration. Cluster II (*glo1*, *mgstt2*, chac2, *mgst3b*): glutathione conjugation and degradation-related genes, showing "up-regulation at low doses, suppression at high doses" and "mid-term up-regulation, suppression at early and late stages". Medium/high doses induced up-regulation at 40 d, but at 60 d almost all were down-regulated. Cluster III (*selenop2*, *gsr*, *hagh*, *selenoo1*): continuously increased in the control at late stages; in supplemented groups, the peak was delayed and later suppressed. Notably, *gsr* was mostly negative throughout in Groups D and E, suggesting that high Se may impair GSH regeneration capacity. The strongest up-regulation peak of all genes occurred in Group C at 40 d.

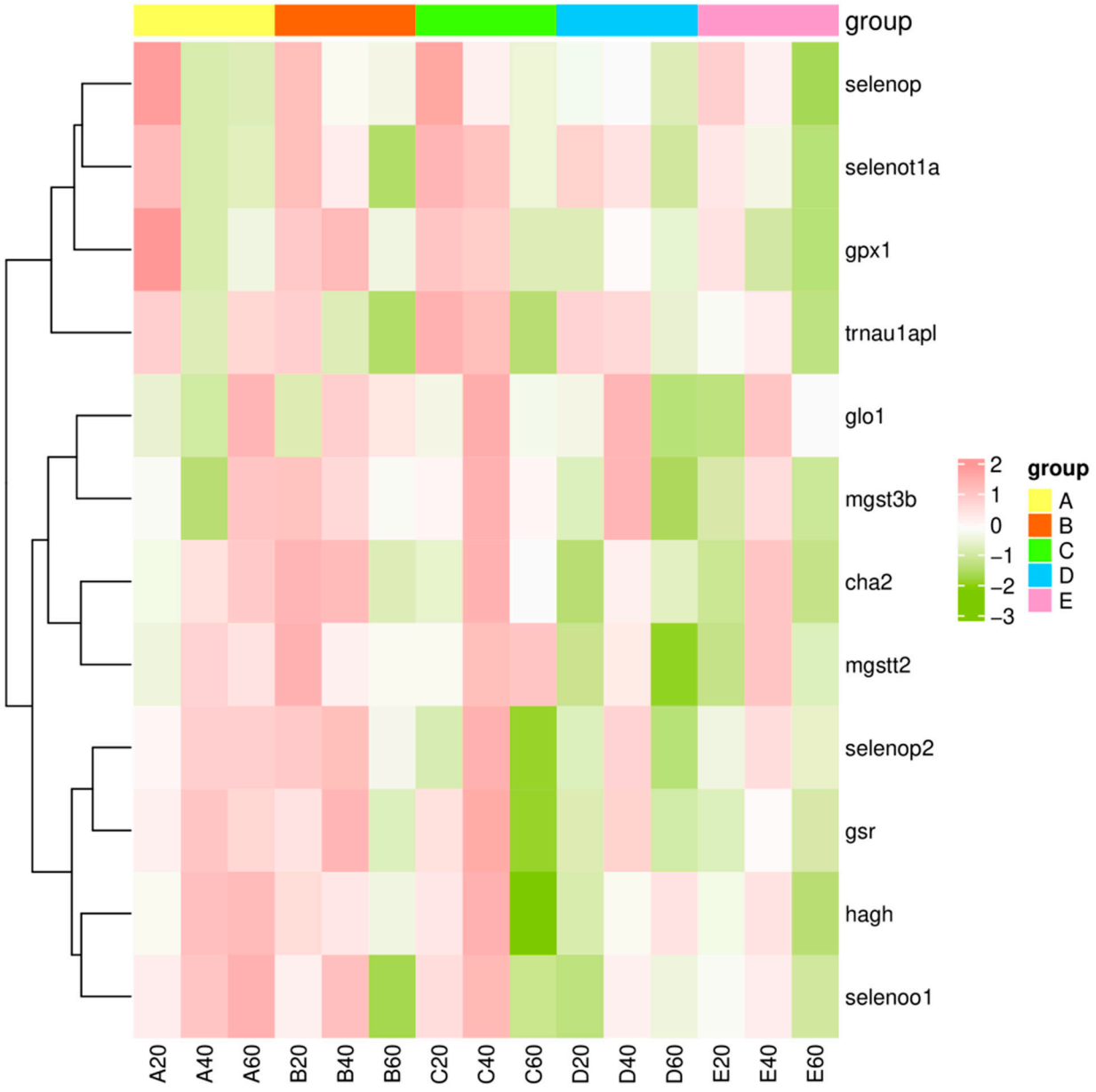


Figure 9. Heatmap clustering of log_2FC of hepatic selenium metabolism-related genes. Rows: indicators; columns: time-concentration combinations. Red, up-regulation; green, down-regulation.

3.5. Correlation Analysis Between Hepatic Biochemical Indices and Key Genes

Global Spearman correlation analysis (45 samples) showed highly significant positive correlations between selenoprotein genes (*selenoo1*, *selenop*, *selenot1a*, *gpx1*) and glutathione metabolism genes (*gsr*, *hagh*, chac2, *mgst3b*) (ϱ = 0.63–0.86, $p < 0.001$). Correlations between selenoprotein genes and antioxidant enzyme activities (GSH-Px, SOD, T-AOC) were weak or negative (e.g., *selenot1a* vs. SOD: $\varrho = -0.342$, $p < 0.05$). Transaminase ALT was strongly positively correlated with *selenop*, *selenot1a*, and *gpx1* (ϱ = 0.66–0.74, $p < 0.001$) (Figure 10).

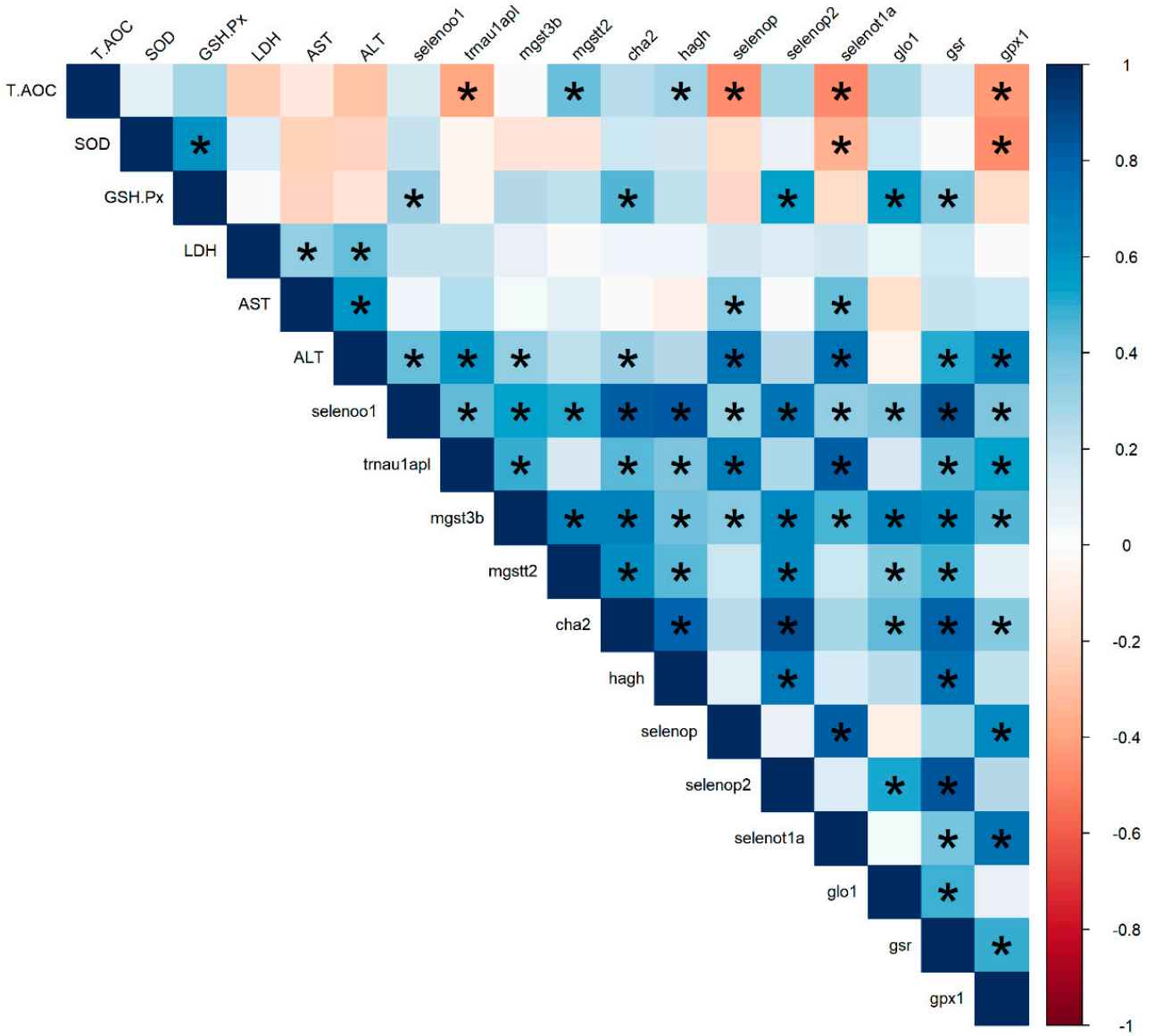


Figure 10. Heatmap of correlations between hepatic biochemical indices and expression of selenium metabolism-related genes. The correlation coefficient between these two factors is represented by the intensity of the color. The color of the rectangles ranges from blue to red, indicating negative correlation (close to −1) to positive correlation (close to 1). *: statistically significant correlations ($p < 0.05$).

3.5.1. Stratification by Concentration

In Group C (1.0 mg Se/kg diet), the gene–enzyme positive correlations were most significant and widespread (e.g., *selenoo1* vs. SOD: $\varrho = 0.90$, $p < 0.001$), indicating the

strongest synergistic regulation at this dose. Weak correlations in Group A, moderate in B and D, and extensive negative correlations in Group E (3.0 mg Se/kg diet) (e.g., *selenot1a* vs. GSH-Px: $\rho = -0.80$, $p < 0.01$) suggest that high dose disrupts positive coupling.

3.5.2. Stratification by Time

Day 40 exhibited the strongest gene–enzyme coupling (e.g., *selenot1a* vs. *glo1*: $\rho = 0.86$, $p < 0.001$). At day 20, most correlations were not significant, indicating that the regulatory network had not yet been established. At day 60, the positive correlation network disintegrated (e.g., *selenoo1* vs. T-AOC: $\rho = -0.73$, $p < 0.01$), reflecting feedback inhibition induced by long-term Se exposure.

4. Discussion

The biological effects of nano-selenium (Nano-Se) are influenced by the interaction between dietary dose and feeding duration, which is difficult to reveal using traditional single-factor experiments. Moreover, current knowledge on Nano-Se in the large-scale loach (*Paramisgurnus dabryanus*) is largely limited to phenotypic parameters such as growth and antioxidant status, while the molecular mechanisms underlying selenium metabolism remain poorly understood. Therefore, this study employed response-surface methodology (RSM) with dietary Nano-Se concentration and feeding duration as two factors, systematically analyzed their interactive effects on growth performance, and combined dynamic changes in hepatic biochemical indices and expression of key selenium metabolism-related genes to explore the dose–time effects of Nano-Se at both phenotypic and molecular levels, aiming to provide a scientific basis for precision selenium nutrition in *P. dabryanus*.

4.1. Dual-Dimensional (Dose–Time) Effects of Nano-Se on Growth Performance and Optimization

The biological effect of selenium follows a typical U-shaped curve, where both deficiency and excess inhibit the growth of aquatic animals [4,8]. Single-factor experiments can only assess the effect of one factor at a time and cannot reveal the interaction between Se concentration and feeding duration. To address this, we established quadratic regression models for WGR and SGR using central composite design (CCD) within RSM. ANOVA showed that the models were highly significant ($p < 0.01$), with non-significant lack-of-fit, and adjusted R^2 values of 0.972 and 0.855, respectively, indicating good fit for prediction and optimization. From the regression coefficients and response-surface plots (Figures 4 and 5), the effects of Nano-Se concentration on both WGR and SGR followed a parabolic trend of first increase then decrease, with the optimal Se level from Nano-Se around 1.0 mg Se/kg diet. Feeding duration had a continuously positive effect on WGR (highest at 60 d), whereas its effect on SGR increased rapidly and then plateaued (no significant difference after 30 d). The plateau in SGR after 30 days may be related to the natural growth pattern of juvenile fish, but the underlying mechanisms were not investigated in this study and require further research. Interaction analysis revealed no significant product effect (TS term, $p > 0.05$), indicating that the effects of Se concentration and feeding duration on growth are relatively independent. Several studies have shown that under sufficient Se supply, selenoprotein expression and enzyme activity can reach a plateau within a short time (hours to days) and then remain stable, rather than continuously increasing linearly with feeding duration [19]. Therefore, the effect of Se on growth mainly depends on whether the optimal dose is achieved, rather than the length of feeding duration. In the present study, growth responses at all time points from 20 to 60 d consistently showed 1.0 mg Se/kg diet as the optimal Se level from Nano-Se (Figure 2).

Based on the RSM results, the optimal Nano-Se addition for juvenile *P. dabryanus* is 1.0 mg/kg, and the optimal feeding duration is 60 d (for maximum weight gain) or 30–40 d (for maximum specific growth rate). This conclusion provides a basis for the selection of sampling time points (20, 40, 60 d) for subsequent biochemical and gene expression analyses. The optimal Nano-Se concentration identified in this study (1.0 mg Se/kg diet) is generally consistent with findings in other freshwater fish species, such as common carp (1–2 mg Se/kg diet) [5], yellow catfish (0.5–1.0 mg Se/kg diet) [15], and grass carp (0.5–1.0 mg Se/kg diet) [14]. However, the optimal feeding duration and the dose–time interaction have rarely been systematically evaluated in previous studies. Our study demonstrates that the effects of Nano-Se concentration and feeding duration on growth are relatively independent, with concentration exerting a stronger influence on SGR and duration on WGR. This finding provides practical guidance for feed formulation: the optimal dietary Nano-Se level should be prioritized, and the feeding duration can be adjusted according to the target production stage (e.g., 30–40 days for maximum SGR or 60 days for maximum weight gain). Moreover, the application of RSM/CCD to optimize both concentration and duration in *P. dabryanus* extends this approach to a new aquaculture species and offers a methodological reference for precision selenium nutrition in other farmed fish. This conclusion also provides a basis for the selection of sampling time points (20, 40, 60 d) for subsequent biochemical and gene-expression analyses.

4.2. Biphasic Regulation of Hepatic Antioxidant System and Metabolic-Enzyme Activities by Nano-Se

In the control group (Group A, 0.0 mg/kg), hepatic T-AOC, SOD, and GSH-Px activities increased continuously with culture time, likely reflecting a compensatory mechanism to maintain antioxidant capacity under basal Se supply to meet growth and metabolic demands [20]. However, the low dose of Nano-Se (Group B, 0.5 mg Se/kg diet) inhibited SOD and GSH-Px activities. This dose may fall within the suboptimal range of the Se U-shaped curve, where Se supply is insufficient to fully activate selenoprotein synthesis; however, the exact mechanisms underlying this inhibition were not investigated in this study and require further research. This phenomenon is consistent with the "low inhibition, high promotion" pattern observed in common carp by Ashouri et al. [5], further confirming the non-monotonic dose dependence of Nano-Se nutritional effects. The medium dose (Group C, 1.0 mg Se/kg diet) maintained stable antioxidant capacity during the mid-culture period and showed a smaller decline in transaminases at later stages, indicating a balance between oxidative stress defense and metabolic homeostasis [10].

High doses of Nano-Se (Groups D and E, 2.0 and 3.0 mg/kg) strongly activated GSH-Px and SOD in the early period, but prolonged feeding (60 d) led to significant decreases in AST and ALT activities. The heatmap further revealed an "uncoupling" phenomenon in Group E60, with large up-regulation of antioxidant enzymes but down-regulation of transaminases, indicating that excessive Se continuously activates selenoprotein synthesis and antioxidant pathways while potentially inhibiting transamination and interfering with normal amino acid metabolism [4]. Similarly, high-dose Nano-Se (1–2 mg Se/kg diet) increased serum transaminase activities in common carp, suggesting liver damage [5]; in yellow catfish, although high Se alleviated oxidative stress induced by oxidized fish oil, long-term exposure also disturbed amino acid metabolism [15]. This is consistent with in vitro studies in rainbow trout hepatocytes, where high exposure to various selenium forms (e.g., selenite or selenomethionine) was shown to induce oxidative stress and exert cytotoxicity via reactive oxygen species generation [21,22]. In contrast, in grass carp, dietary Nano-Se supplementation reduced transaminase levels and improved liver health, exerting a hepatoprotective effect [14]. Furthermore, Se deficiency has been shown to reduce glutathione peroxidase activity in fish, weakening antioxidant capacity and leading

to free-radical accumulation. Studies have indicated that Se serves as the active center of GSH-Px, playing important roles in metabolism and various physiological activities in aquatic animals, although excess Se can also cause toxicity [13]. As a selenium source additive and free radical scavenger, Nano-Se demonstrates unique protective effects against environmental heat stress in rainbow trout, significantly increasing liver GPx activity and up-regulating GPx1a gene expression levels [13]. In summary, the antioxidant-metabolism axis "uncoupling" induced by high-dose Nano-Se may mark the transition from beneficial to toxic effects of Se, further confirming the extremely narrow range between dietary essentiality and toxicity of Se in aquatic organisms [23].

4.3. Effects of Nano-Se on Key Gene Expression in Selenium Metabolism and Molecular Mechanisms

This study revealed three distinct response patterns based on expression dynamics of 12 selenoprotein and glutathione metabolism-related genes in the liver [24]. Cluster I genes (*selenop*, *selenot1a*, *gpx1*, *trnau1ap*) exhibited a dynamic pattern of "early transient up-regulation in control, mid-term induction peak, and late dose-dependent suppression" in the liver of *P. dabryanus*. These genes are directly involved in selenoprotein synthesis or encode selenoproteins themselves. Among them, *trnau1ap* (SECp43) is an upstream key assembly factor for the selenoprotein translation machinery, directly regulating the efficiency of co-translational selenocysteine insertion [25,26]; *selenop*, *selenot1a*, and *gpx1* encode selenoprotein P, selenoprotein T1a, and glutathione peroxidase 1, respectively, performing antioxidant, selenium transport, and redox regulatory functions [27]. The four genes shared a highly consistent three-stage dynamic: Early transient up-regulation in control (A20): Under basal Se levels (without exogenous Nano-Se supplementation), the fish transiently up-regulated *selenop*, *selenot1a*, *gpx1*, and *trnau1ap* to optimize the utilization of limited Se resources and maintain basal selenoprotein function and redox balance [28]. This is consistent with the strategy in mammals of prioritizing essential selenoprotein expression during Se deficiency [25,27] and reflects adaptive responses in fish under inadequate Se supply. Mid-term induction peak (20–40 d): In the Nano-Se supplemented groups, the degree of induction was positively correlated with Se dose within a certain range, but peak timing and dose dependence varied among genes: *selenot1a* and *gpx1* remained highly expressed from 20 to 40 d, while *trnau1ap* and *selenop* began to decline soon after the 20 d induction. This reflects a "priority hierarchy" in selenoprotein synthesis: the genes directly involved in antioxidant defense (*gpx1* and *selenot1a*) are translated first, while the Se transporter *selenop* is subject to tighter feedback control. Pacitti et al. (2013) [29] found in rainbow trout hepatocytes that GPx1 isoforms, particularly GPx1a, showed the highest sensitivity to selenium availability in vitro, suggesting that GPx1 transcript expression level may serve as a sensitive biomarker for selenium intake. Conversely, studies in fish have demonstrated that appropriate Nano-Se supplementation can restore the expression of selenoprotein synthesis-related genes (e.g., GPx) under stress conditions [13,14], indirectly supporting the hierarchical regulation of selenoprotein expression. Late-stage dose-dependent suppression (60 d): at 60 d, almost all Cluster I genes in supplemented groups were suppressed, and the degree of suppression was positively correlated with Nano-Se dose (E60 > D60 > C60 > B60). The core mechanism of this global negative feedback is the down-regulation of *trnau1ap* (SECp43), acting as a "master switch" for selenoprotein translation, thereby blocking the synthesis of downstream selenoproteins (including *selenop*, *selenot1a*, *gpx1*). When hepatic Se reserves remain high for a long period, the organism suppresses *trnau1ap* expression to fundamentally reduce selenoprotein synthesis, avoiding excessive Se consumption and potential Se toxicity (e.g., protein dysfunction through non-specific sulfur substitution, excessive ROS generation) [30]. This negative feedback mechanism is supported by studies in fish: high-dietary Se levels have

been shown to down-regulate the expression of trnau1ap and related selenoprotein genes in yellow catfish [15], and supra-nutritional doses of dietary selenium have been reported to inhibit hepatic selenoprotein gene expression in rainbow trout [13]. These findings are highly consistent with the present results, confirming that excessive Se supply triggers a conserved negative regulatory loop that limits selenoprotein synthesis to prevent Se toxicity.

Cluster II genes (*glo1*, *mgstt2*, chac2, *mgst3b*) all function in a glutathione (GSH)-dependent manner, constituting a GSH-dependent secondary defense module that compensates for maintaining redox balance when selenoprotein function is limited. Glutathione is a bioactive peptide widely present in cells, playing important roles in antioxidant defense, immune response, and detoxification. Fish glutathione S-transferases (GSTs) are important phase II detoxification enzymes that play key roles in catalyzing the conjugation of toxins with reduced glutathione. The genes in this cluster showed "dose- and time-dependent bidirectional regulation": up-regulation at moderate doses or in the mid-phase (e.g., 40 d), but mostly suppression at high doses or long-term (60 d) exposure [31]. This dynamic is similar to that of Cluster I genes, but the sensitivity to dose/time varies among different genes. Early suppression (20 d): In A20, B20, C20, D20, E20, *glo1*, *mgst3b*, and chac2 were almost all negative, while only *mgstt2* remained up-regulated in B20 and C20. This suggests that early in Nano-Se exposure, the organism prioritizes Cluster I selenoproteins (*selenot1a*, *gpx1*, etc.) for antioxidant functions, and may allocate limited GSH resources to selenoprotein synthesis and GPx reactions. Mid-term induction (40 d): all four genes showed clear up-regulation peaks at A40, B40, C40, D40, and E40. This "mid-term induction peak" was synchronized with that of Cluster I, but the induction of Cluster II was more concentrated at 40 d. It suggests that after selenoprotein synthesis is fully initiated, the organism further enhances the GSH-dependent secondary defense module to synergistically clear secondary oxidative damage and glycation products generated during Se metabolism. Indeed, studies have shown that dietary Nano-Se supplementation significantly increases hepatic glutathione S-transferase (GST) activity in grass carp fed a high-fat diet [32], and nano-Se has been reported to up-regulate the expression of selenoprotein-related genes, including GPx1a and Trx, in rainbow trout [13], consistent with the 40 d induction peak of Cluster II in this study.

Cluster III genes (*selenop2*, *gsr*, *hagh*, *selenoo1*) mainly function in the GSH regeneration cycle (*gsr*), subsequent metabolism of GSH-conjugated products (*hagh*), and some special members of the selenoprotein family (*selenop2*, *selenoo1*). Among them, *mgst3b* (microsomal glutathione S-transferase 3b) is predicted to enable glutathione peroxidase activity and glutathione transferase activity, primarily localized in the endoplasmic reticulum and nuclear envelope. They showed a highly consistent pattern of "continuous increase in the control, delayed peak (or phase shift) in supplemented groups, and suppression at high doses/long term". In the control group: the $\log_2$FC of all four genes continuously increased from negative or near-zero to moderately positive values, indicating that without exogenous Nano-Se, the endogenous Se reserve may be insufficient, and the organism continuously up-regulates *gsr*, *hagh*, and certain selenoproteins (*selenop2*, *selenoo1*) to maximize the use of limited Se resources and maintain GSH cycling and redox balance [33]. This is consistent with the compensatory up-regulation of *gsr* and *hagh* under Se deficiency in mammals [25,27] and also reflects a high dependence on the GSH regeneration pathway in fish under low-Se status [34]. In supplemented groups (B, C, D, E): when exogenous Se is adequate, the peak of this module does not appear at 20 d but is delayed to 40 d (B40, C40) or even 60 d (e.g., *hagh* trends at B60, C60). This "peak delay" likely reflects a "priority strategy" after Se supplementation: first, meet the synthetic demands of Cluster I selenoproteins (direct antioxidants and Se transporters), and only later induce auxiliary systems such as GSR and HAGH. This is consistent with our observation that Cluster

I genes were already strongly induced at 20 d, while the significant rise of Cluster III genes generally occurred at 40 d and beyond. In line with this, studies in other fish species have shown that dietary selenium levels can significantly regulate the expression of multiple selenoprotein genes, including GPX1, GPX4, and SELENOP [35]; and Pacitti et al. (2013) [29] similarly found that GPx1 responded most rapidly to Se in rainbow trout hepatocytes, whereas other selenoprotein genes showed delayed expression. Together, these findings support the inferred "priority hierarchy" of selenoprotein expression.

4.4. Dose- and Time-Dependent Correlation Patterns Between Hepatic Biochemical Indices and Key Genes

Spearman correlation analysis showed that under Nano-Se treatment, selenoprotein genes (*selenop*, *selenot1a*, *gpx1*, *selenoo1*) were highly significantly positively correlated with glutathione metabolism-related genes (*gsr*, *hagh*, chac2, *mgst3b*, *mgstt2*) ($\varrho = 0.63–0.86$, $p < 0.001$), indicating widespread transcriptional co-regulation between selenoprotein synthesis and GSH-dependent secondary detoxification systems [36]. However, correlations between selenoprotein genes and antioxidant enzyme activities (GSH-Px, SOD, T-AOC) were weak or negative (e.g., *selenot1a* vs. SOD: $\varrho = -0.342$, $p < 0.05$), suggesting an uncoupling between transcription and enzyme activity. Stratification by concentration revealed that Group C (1.0 mg Se/kg diet) exhibited the strongest and most extensive positive gene–enzyme correlations (e.g., *selenoo1* vs. SOD: $\varrho = 0.90$, $p < 0.001$), representing the optimal dose. Correlations were weak in Group A (control), moderate in Groups B and D, and extensively negative in Group E (3.0 mg Se/kg diet) (e.g., *selenot1a* vs. GSH-Px: $\varrho = -0.80$, $p < 0.01$), indicating that high dose disrupts positive coupling. Stratification by time showed that day 40 was the period of strongest gene–enzyme coupling (e.g., *selenot1a* vs. *glo1*: $\varrho = 0.86$, $p < 0.001$); no significant correlations were observed at day 20, indicating that the regulatory network had not yet been established; at day 60, the positive correlation network disintegrated (e.g., *selenoo1* vs. T-AOC: $\varrho = -0.73$, $p < 0.01$), reflecting feedback inhibition induced by long-term Se exposure [37]. In summary, the regulatory effect of Nano-Se is both concentration- and time-dependent: 1.0 mg/kg for 40 d is the optimal synergistic window, whereas high dose (3.0 mg/kg) or long-term (60 d) exposure leads to transcription-enzyme activity uncoupling and negative correlations, possibly related to NADPH consumption, suppression of *trnau1ap* expression, and oxidative damage induced by Se toxicity [15]. It should be noted that the correlation analysis treated the 15 treatment–time combinations as independent observations, whereas repeated measurements from the same concentration group may not be fully independent. Therefore, the correlation results should be interpreted as exploratory, and the stratified analyses by concentration and time provide more robust support for the main conclusions.

5. Conclusions

This study demonstrates that response-surface methodology is an effective tool for optimizing dietary Nano-Se supplementation in juvenile *P. dabryanus*. The optimal growth was achieved at 1.0 mg Se/kg diet Nano-Se, while feeding duration had an independent effect: WGR increased continuously with time, whereas SGR plateaued after 30 days. Nano-Se exhibited a non-monotonic, dose-dependent effect on hepatic antioxidant capacity. The medium dose (1.0 mg Se/kg diet) at 40 days showed the strongest gene–enzyme coupling, representing the optimal synergy window. In contrast, the low dose (0.5 mg Se/kg diet) suppressed antioxidant enzymes, and the high dose (3.0 mg Se/kg diet) caused transcriptional-enzymatic uncoupling, indicating a narrow safe range for Se supplementation. At the molecular level, 12 functional genes were classified into three clusters, revealing a hierarchical priority in selenoprotein translation: antioxidant-defense genes (*gpx1*, *selenot1a*) were prioritized under adequate Se supply, while *trnau1ap* (SECp43)

was globally down-regulated under long-term high-Se exposure, acting as a potential master switch for selenoprotein synthesis. In conclusion, the optimal Nano-Se supplementation for juvenile *P. dabryanus* is 1.0 mg Se/kg diet for 40 days (or 60 days for maximum weight gain), providing a theoretical basis for precision selenium nutrition in farmed fish.

Supplementary Materials: The following supporting information can be downloaded at: https://www.mdpi.com/article/10.3390/antiox15111392/s1, Figure S1: geNorm analysis of candidate reference gene stability; Figure S2: Standard curve parameters of reference genes; Table S1: Factors and levels for central composite design; Table S2: Sequences of primers used for qRT-PCR, amplification efficiency, slope, and R^2; Table S3: Central composite design results (WGR); Table S4: Analysis of mean square on the activities of WGR; Table S5: Central composite design results (WGR); Table S6: Analysis of mean square on the activities of SGR.

Author Contributions: Z.H.: Conceptualization, data curation, investigation, methodology, software, writing—original draft. B.M.: Methodology, software, validation. X.W.: Data curation, investigation, methodology. R.D.: Methodology, data curation. Q.L.: Methodology, data curation. H.W. and A.M.: Funding acquisition, project administration, writing—review and editing. G.Y.: Data curation. G.K.: Resources, validation. All authors have read and agreed to the published version of the manuscript.

Funding: This research was funded by the Major Discipline Academic and Technical Leaders Training Program of Jiangxi Province (grant numbers 20225BCJ22017); China Agriculture Research System of MOF and MARA (grant numbers CARS-47-G01); the Modern Agricultural Industry Technology System of Jiangxi Province (grant numbers JXARS-15); and Central Public-interest Scientific Institution Basal Re-search Fund, CAFS (grant numbers 2023TD26).

Institutional Review Board Statement: The animal study protocol was approved by the Experimental Animal Ethics Committee of Yellow Sea Fisheries Research Institute, Chinese Academy of Fishery Sciences (Decision No: YSFRI-2025079, approval on 11 November 2025).

Informed Consent Statement: Not applicable.

Data Availability Statement: The raw data supporting the conclusions of this article will be made available by the authors on request.

Conflicts of Interest: Guohua Ke is from Jiujiang Xingxiang Aquatic Breeding Co., Ltd. The company had no role in the design of the study; in the collection, analyses, or interpretation of data; in the writing of the manuscript; or in the decision to publish the results. All other authors declare no conflicts of interest.

References

1. Dawood, M.A.O.; El-Basuini, M.F.; Yilmaz, S.; Abdel-Latif, H.M.R.; Kari, Z.A.K.; Razab, M.K.A.A.; Ahmed, H.A.; Alagawany, M.; Gewaily, M.S.G. Selenium Nanoparticles as a Natural Antioxidant and Metabolic Regulator in Aquaculture: A Review. *Antioxidants* **2021**, *10*, 1364.
2. Khalil, H.S.; Maulu, S.; Verdegem, M.; Abdel-Tawwab, M. Embracing Nanotechnology for Selenium Application in Aquafeeds. *Rev. Aquac.* **2023**, *15*, 112–129.
3. Ahmed, S.R.; Van Doan, H.; Davies, S.; Hassaan, M.S.; Goda, A.M.A.; EI-Haroun, E. Effect of Selenium and Nano-Selenium Applications on Biological Functions in Aquaculture—A Review. *Ann. Anim. Sci.* **2025**, *25*, 905–919.
4. Hamilton, S.J. Review of Selenium Toxicity in the Aquatic Food Chain. *Sci. Total Environ.* **2004**, *326*, 1–31.
5. Ashouri, S.; Keyvanshokooh, S.; Salati, A.P.; Johari, S.A.; Pasha-Zanoosi, H. Effects of Different Levels of Dietary Nano-Selenium on Growth Performance, Carcass Composition, Blood Biochemical Parameters, and Antioxidant Status in Common Carp (*Cyprinus carpio*). *Aquaculture* **2015**, *446*, 25–29.

6. Berntssen, M.H.G.; Sundal, T.K.; Olsvik, P.A.; Amlund, H.; Rasinger, J.D.; Sele, V.; Hamre, K.; Hillestad, M.; Buttle, L.; Ørnsrud, R. Sensitivity and Toxic Mode of Action of Dietary Organic and Inorganic Selenium in Atlantic Salmon (*Salmo salar*). *Aquat. Toxicol.* **2017**, *192*, 116–126.
7. Fillipa-Silva, A.; Monteiro, M.; Costa, R.S.; Sa, T.; Marques, A.; Valente, L.M.P.; Figueiredo-Silva, C. Comparative study of dietary selenium sources on gilthead seabream (*Sparus aurata*): Growth, nutrient utilization, stress response and final product quality. *Aquaculture* **2025**, *595*, 741508.
8. Le, K.T.; Fotedar, R. Bioavailability of selenium from different dietary sources in yellowtail kingfish (*Seriola lalandi*). *Aquaculture* **2014**, *420–421*, 57–62.
9. Zahran, E.; Wang, B.; Amoah, K.; Elbahnaswy, S.; Ahmed, F.; Farid, O.A.A.; Risha, E.; Eldesoqui, M.; El, S.; Mahmoud, G.; et al. Dietary Selenium Nanoparticles (SeNPs) Mediate Intestinal Microbiome and Microbiota-Derived Metabolites Regulating the Growth and Immunity of Nile Tilapia. *J. World Aquac. Soc.* **2025**, *56*, e70019. Correction in *J. World Aquac. Soc.* **2025**, *56*, e70057.
10. Wang, L.; Xiao, J.X.; Hua, Y.; Xiang, X.W.; Zhou, Y.F.; Ye, L.; Shao, Q.J. Effects of Dietary Selenium Polysaccharide on Growth Performance, Oxidative Stress and Tissue Selenium Accumulation of Juvenile Black Sea Bream, *Acanthopagrus schlegelii*. *Aquaculture* **2019**, *503*, 389–395.
11. Hu, Y.; Liu, Y.; Ma, A.J.; Wang, H.H.; Sun, Z.B.; Jiang, Y.H.; Cao, J.W.; Zhang, H.; Huang, Z.H.; Ma, B.H. Early Body Colour Development and Related Genes Expression Analysis of Selected Strain "Ganhong No.1" and *Paramisgurnus dabryanus* ssp. *taiwanensis*. *Oceanol. Limnol. Sin.* **2025**, *56*, 214–225.
12. Huang, Z.; Wang, X.; Ma, B.; Deng, R.; Gao, Y.; Yu, G.; Ke, C.; Wang, H.; Ma, A. Genotype by Selenium Concentration Interactions for Selenium-Related Genes in Paramisgurnus dabryanus at Different Durations. *Animals* **2026**, *16*, 2837.
13. Li, L.; Liu, Z.; Quan, J.; Lu, J.; Zhao, G.; Sun, J. Dietary Nanoselenium Supplementation for Heat-Stressed Rainbow Trout: Effects on Organizational Structure, Lipid Changes, and Biochemical Parameters as Well as Heat-Shock-Protein- and Selenoprotein-Related Gene Expression. *Fish Physiol. Biochem.* **2022**, *48*, 707–722.
14. Ye, L.M.; Liu, S.; Zhang, X.T.; Wang, C.; Li, P.J.; Zhang, C.; Ji, H.; Yu, H.B. Dietary Nano-Selenium Improves Health of Liver and Intestine of Grass Carp (*Ctenopharyngodon idella*) after Overwintering. *Aquaculture* **2023**, *306*, 115817.
15. Liu, G.H.; Zhang, D.G.; Lei, X.J.; Tan, X.Y.; Song, C.C.; Zheng, H.; Luo, Z. Effects of Dietary Selenium and Oxidized Fish Oils on Intestinal Lipid Metabolism and Antioxidant Responses of Yellow Catfish *Pelteobagrus fulvidraco*. *Antioxidants* **2022**, *11*, 1904.
16. Shang, X.C.; Che, X.H.; Geng, L.W.; Zhang, Q.; Wei, H.J.; Shi, X.D.; Xu, W. Transcriptomic analysis reveals that selenium-enriched Lactobacillus plantarum alleviates high-salinity stress in common carp through lipid metabolism and ferroptosis signalling pathways. *Ecotoxicol. Environ. Saf.* **2025**, *302*, 118690.
17. Grunow, B.; Strauch, S.M. Status assessment and opportunities for improving fish welfare in animal experimental research according to the 3R-Guidelines. *Rev. Fish Biol. Fish.* **2023**, *33*, 1075–1093.
18. Hellemans, J.; Vandesompele, J. Selection of Reliable Reference Genes for RT-qPCR Analysis. In *Quantitative Real-Time PCR: Methods and Protocols*; Springer: New York, NY, USA, 2014; pp. 19–26.
19. Lin, Y.H.; Shiau, S.Y. Dietary Selenium Requirements of Juvenile Grouper, *Epinephelus malabaricus*. *Aquaculture* **2005**, *250*, 356–363.
20. Surai, P.F. *Selenium in Nutrition and Health*; Nottingham University Press: Nottingham, UK, 2006; ISBN 190476116X.
21. Misra, S.; Hamilton, C.; Niyogi, S. Induction of Oxidative Stress by Selenomethionine in Isolated Hepatocytes of Rainbow Trout (*Oncorhynchus mykiss*). *Toxicol. In Vitro* **2012**, *26*, 621–629.
22. Misra, S.; Niyogi, S. Selenite Causes Cytotoxicity in Rainbow Trout (*Oncorhynchus mykiss*) Hepatocytes by Inducing Oxidative Stress. *Toxicol. In Vitro* **2009**, *23*, 1249–1258.
23. Lemly, A.D. Guidelines for Evaluating Selenium Data from Aquatic Monitoring and Assessment Programs. *Environ. Monit. Assess.* **1993**, *28*, 83–100.
24. Mariotti, M.; Ridge, P.G.; Zhang, Y.; Lobanov, A.V.; Pringle, T.H.; Guigo, R.; Hatfield, D.L.; Gladyshev, V.N. Composition and Evolution of the Vertebrate and Mammalian Selenoproteomes. *PLoS ONE* **2012**, *7*, e33066.
25. Pillai, R.; Uyehara-Lock, J.H.; Bellinger, F.P. Selenium and Selenoprotein Function in Brain Disorders. *IUBMB Life* **2014**, *66*, 229–239.
26. Papp, L.V.; Lu, J.; Holmgren, A.; Khanna, K.K. From Selenium to Selenoproteins: Synthesis, Identity, and Their Role in Human Health. *Antioxid. Redox Signal.* **2007**, *9*, 775–806.
27. Burk, R.F.; Hill, K.E. Regulation of Selenium Metabolism and Transport. *Annu. Rev. Nutr.* **2015**, *35*, 109–134.
28. Sunde, R.A.; Raines, A.M. Selenium Regulation of the Selenoprotein and Nonselenoprotein Transcriptomes in Rodents. *Adv. Nutr.* **2011**, *2*, 138–150.

29. Pacitti, D.; Wang, T.; Martin, S.A.M.; Sweetman, J.; Feldmann, J.; Secombes, C.J. Characterization of Cytosolic Glutathione Peroxidase and Phospholipid-Hydroperoxide Glutathione Peroxidase Genes in Rainbow Trout (*Oncorhynchus mykiss*) and Their Modulation by In Vitro Selenium Exposure. *Aquat. Toxicol.* **2013**, *130–131*, 97–111.
30. Labunskyy, V.M.; Hatfield, D.L.; Gladyshev, V.N. Selenoproteins: Molecular Pathways and Physiological Roles. *Physiol. Rev.* **2014**, *94*, 739–777.
31. Hayes, J.D.; Flanagan, J.U.; Jowsey, I.R. Glutathione Transferases. *Annu. Rev. Pharmacol. Toxicol.* **2005**, *45*, 51–88.
32. Yu, H.B.; Zhang, C.; Zhang, X.T.; Wang, C.; Li, P.; Liu, G.; Yan, X.; Xiong, X.; Zhang, L.; Hou, J.Y.; et al. Dietary Nano-Selenium Enhances Antioxidant Capacity and Hypoxia Tolerance of Grass Carp (*Ctenopharyngodon idella*) Fed with High-Fat Diet. *Aquac. Nutr.* **2020**, *26*, 545–557.
33. Lu, S.C. Glutathione Synthesis. *Biochim. Biophys. Acta Gen. Subj.* **2013**, *1830*, 3143–3153.
34. Pacini, N.; Abete, M.C.; Dörr, A.J.M.; Prearo, M.; Natali, M.; Elia, A.C. Detoxifying Response in Juvenile Tench Fed by Selenium Diet. *Environ. Toxicol. Pharmacol.* **2012**, *33*, 46–52.
35. Chen, Z.; Liu, H.K.; Liu, C.; Fei, S.Z.; Hu, X.M.; Han, D.; Jin, J.Y.; Yang, Y.X.; Zhu, X.M.; Xie, S.Q. Effects of Different Dietary Selenium Sources on the Meat Quality and Antioxidant Capacity of Yellow Catfish (*Pelteobagrus fulvidraco*). *Aquac. Nutr.* **2023**, *2023*, 7981183.
36. Gladyshev, V.N.; Arnér, E.S.; Berry, M.J.; Brigelius-Flohé, R.; Bruford, E.A.; Burk, R.F.; Carlson, B.A.; Castellano, S.; Chavatte, L.; Conrad, M. et, al. Selenoprotein Gene Nomenclature. *J. Biol. Chem.* **2016**, *291*, 24036–24040.
37. Lushchak, V.I. Environmentally Induced Oxidative Stress in Aquatic Animals. *Aquat. Toxicol.* **2011**, *101*, 13–30.

Disclaimer/Publisher's Note: The statements, opinions and data contained in all publications are solely those of the individual author(s) and contributor(s) and not of MDPI and/or the editor(s). MDPI and/or the editor(s) disclaim responsibility for any injury to people or property resulting from any ideas, methods, instructions or products referred to in the content.